TECHNICAL REPORT STANDARD TITLE PAGE

1. Report No.	2. Government Accession No.	3. Recipient's Catalog No.
CFHR 3-5-75-172-1		

4. Title and Subtitle	5. Report Date
AXIAL TENSION FATIGUE STRENGTH OF ANCHOR BOLTS	March 1977
	6. Performing Organization Code
7. Author(s)	8. Performing Organization Report No.
Franklin L. Fischer and Karl H. Frank	Research Report Number 172-1
9. Performing Organization Name and Address	10. Work Unit No.
Center for Highway Research The University of Texas at Austin Austin, Texas 78712	11. Contract or Grant No. Research Study 3-5-75-172
	13. Type of Report and Period Covered
12. Sponsoring Agency Name and Address Texas State Department of Highways and Public Transportation; Transportation Planning Division P. O. Box 5051 Austin, Texas 78763	Interim
	14. Sponsoring Agency Code

15. Supplementary Notes

Work done in cooperation with the Department of Transportation, Federal Highway Administration.
Research Study Title: "Mechanical and Fatigue Behavior of High Strength Anchor Bolts"

16. Abstract

This report presents the results of an experimental investigation to determine the influence of several specification and design parameters on the fatigue behavior of commonly used anchor bolts. The parameters studied include: type of steel, thread series, nominal diameter, thread forming method, and stress range on the tensile stress area.

Analysis of the test results showed that the fatigue life of anchor bolts is comparable to a Category E detail in the present AASHTO fatigue specifications. The pitch of the thread and the diameter of the anchor bolt did not influence the fatigue behavior of the bolts studied. The tensile strength of the steel did influence the fatigue life of the anchor bolts. The A36 steel bolts gave significantly longer fatigue lives. The test series of anchor bolts with rolled threads yielded fatigue lives comparable to bolts with cut threads except at the lower stress ranges. No cracking of the rolled threaded bars was found for stress ranges of 10 and 15 ksi. Longitudinal beam ultrasonic inspection of anchor bolts was found to be capable of detecting early stages of fatigue cracking. A method of estimating the remaining fatigue life of a bolt with a fatigue crack was developed.

17. Key Words	18. Distribution Statement
axial tension, fatigue strength, anchor bolts, stress range, rolled threads, cut threads, tensile strength	No restrictions. This document is available to the public through the National Technical Information Service, Springfield, Virginia 22161.

19. Security Classif. (of this report)	20. Security Classif. (of this page)	21. No. of Pages	22. Price
Unclassified	Unclassified	115	

Form DOT F 1700.7 (8-69)

AXIAL TENSION FATIGUE STRENGTH OF ANCHOR BOLTS

by

Franklin L. Fischer and Karl H. Frank

Research Report 172-1

Project 3-5-75-172
Mechanical and Fatigue Behavior of High Strength Anchor Bolts

Conducted for

Texas
State Department of Highways and Public Transportation

In Cooperation with the
U. S. Department of Transportation
Federal Highway Administration

by

CENTER FOR HIGHWAY RESEARCH
THE UNIVERSITY OF TEXAS AT AUSTIN

March 1977

S U M M A R Y

This report presents the results of an experimental investigation sponsored by the Texas Department of Highways and Public Transportation to determine the influence of several specification and design parameters on the fatigue behavior of commonly used anchor bolts. The parameters studies include: type of steel, thread series, nominal diameter, thread forming method, and stress range on the tensile stress area.

Specimens were 38 in. long with a 6 in. thread on each end and were fabricated from A36, A193 Gr. B7, and 4340 heat treated steel in nominal diameters from 1-3/8 in. to 2 in. Thread series investigated were 8UN, 6UNC, and 4-1/2UNC, with a direct comparison of 8UN versus 6UNC thread series. Also, rolled versus cut threads in the 8UN series were studied and all threads were measured to determine the actual tolerance of fit and the effect on bolt behavior.

All specimens were tested in uniaxial tension under sinusoidal cyclic loading utilizing a 50 cu. in. pulsator and a 200 ton center-hole hydraulic ram. The main experimental variable was stress range.

Ultrasonic inspection during the testing was used to determine initiation and extent of cracking of the specimen with respect to load cycles.

The specimens were tested in a factorial experiment design and the results were analyzed statistically to determine the significance of the above parameters on the fatigue life of the anchor bolts tested.

Analysis of the test results showed that the fatigue life of anchor bolts is comparable to a Category E detail in the present AASHTO fatigue specifications. The pitch of the thread and the

diameter of the anchor bolt did not influence the fatigue behavior of the bolts studied. The tensile strength of the steel did influence the fatigue life of the anchor bolts. The A36 steel bolts gave significantly longer fatigue lives. The test series of anchor bolts with rolled threads yielded fatigue lives comparable to bolts with cut threads except at the lower stress ranges. No cracking of the rolled threaded bars was found for stress ranges of 10 and 15 ksi. Longitudinal beam ultrasonic inspection of anchor bolts was found to be capable of detecting early stages of fatigue cracking. A method of estimating the remaining fatigue life of a bolt with a fatigue crack was developed.

IMPLEMENTATION

This report contains the results of axial tension fatigue tests of anchor bolts with single nuts. The results show that there is no advantage in using high strength anchor bolts from a fatigue standpoint. High strength bolts consistently yielded lower fatigue lives than A36 steel bolts. The fatigue life of the bolts was found to be comparable to that of a Category E detail in the AASHTO fatigue specifications. Future tests will provide information on the influence of double nuts, leveling nut and top nut, on the fatigue life. The present results should be a lower bound to the fatigue life of double nutted bolts and, consequently, provide conservative data for design.

The influence of thread fit upon fatigue life was not found to be systematic. An oversizing of 0.033 in. on galvanized nuts used with galvanized bolts that meet ANSI minimum uncoated thread tolerances was found to be satisfactory.

Ultrasonic inspection using a longitudinal beam provides a rapid and sensitive means of detecting fatigue cracks in anchor bolts and is recommended for field inspection. A means of estimating remaining fatigue life and inspection intervals is given in the report.

CONTENTS

LIST OF TABLES

LIST OF FIGURES

Figure | Page

CHAPTER 1

INTRODUCTION

1.1 Objectives

The fatigue strength of anchor bolts used in highway structures is becoming increasingly significant both in the design of new structures and in the safety and serviceability of existing installations.[12] Bolts used to anchor bridge elements, sign posts, luminaires, lighting towers, and other structures subjected to fluctuations in load should be designed to perform safely and economically under these dynamic loadings throughout the design life of the structure.

The phenomenon of fatigue may generally be defined as the initiation and propagation of cracks which begin at the crystalline level of the material and grow into larger cracks which progress through the material. This crack initiation and growth occurs under repeated applications of stress that may often be considered well below the static capacity of the bolt. As the crack propagates, the cross section of the load-carrying area is reduced resulting in eventual structural failure.[5]

In order to safely and economically design against structural fatigue failures of anchor bolts, the designer must couple loading and life requirements with material properties, thread details, and fabrication quality. Previous investigations of the fatigue strength of threaded connections[6,7,8,13] have indicated that the type of steel; nominal diameter; thread details such as relative thread stiffness, thread pitch, root radius, fit tolerances, stress distribution within the nut, and thread forming method; and stress conditions of maximum stress, minimum stress, stress range and stress ratio all have an effect on fatigue strength.

Although some investigations have considered a range of bolt diameters, most previous work has been done with standard machine bolts and studs within a diameter range of 3/8 in. to 1 in. However, for most highway structures, anchor bolts are commonly fabricated from rolled bar stock in sizes from 1 to 2 in. in diameter. Also, in most investigations reviewed, the systematic evaluation of the various parameters for significance and interaction was minimal.

The objective of this investigation was to determine systematically the primary parameters which affect the fatigue life of commonly used anchor bolts. To reach this objective, 36 anchor bolts were fabricated and tested during the course of the project. The results of these tests were systematically analyzed for significance and interaction of controlled experimental variables. To supplement this objective, full-size static pullout tests were performed to determine the ultimate load capacity for each specimen type. Also Charpy V-notch tests were used to determine the fracture toughness for all steels tested as a function of temperature.

1.2 Experiment Design

The experimental fatigue testing program was structured using a factorial design so that a limited number of specimens could be tested in such a way to give maximum return of significant data. Because of this relatively small sample size and the inherent scatter accompanying fatigue data, the experiment was designed to use satistical methods of analysis to determine, within desired confidence limits, the significance and interaction of controlled variables.

1.2.1 Test Variables. Previous investigations indicated five major factors affect the fatigue strength and life of threaded connections:

(1) Steel type
(2) Nominal Diameter
(3) Thread Type

(4) Thread forming method

(5) Nominal stress

This study included anchor bolts made from three types of steel: A193 Grade B7, A36, and heat treated AISI 4340. These steels give a range in minimum yield stress from 36 ksi for A36 to 150 ksi for the 4340 with an intermediate value of 105 ksi for the A193 Gr. B7 steel. Typically, A36 steel is used for light load anchoring and A193 Gr. B7 and 4340 steels are utilized when large loading capacities are required. All A36 specimens with cut threads were specified to be galvanized according with ASTM standard A153, Class C. The A36 specimens with rolled threads were left uncoated.

Three different diameters, 1-3/8 in., 1-3/4 in., and 2 in. were used in the study with a majority of the specimens being 1-3/8 in. in diameter. Diameters were varied within both high and low strength steel types.

Three thread series were investigated in this study: 8UN, 6UNC, and 4-1/2UNC. These thread series represent typical sizes specified and used for anchor bolt applications in highway structures. In the experiment design standard UNC threads were compared to 8UN series threads to determine the effect of thread size on fatigue behavior. In addition to thread series, clearances of galvanized threads were measured and correlated to test results to determine the effect of thread fit. All nongalvanized threads were specified to conform to American National Standard for Screw Threads (ANSI B1.1), class 2A fit.[2] Also included in this study were the effects of two thread forming methods used in bolt fabrication. Specimens with rolled threads and cut threads were compared inside one factorial group of identical steel, nominal diameter, and loading.

The stress variable selected for the experiment was stress range. This variable was applied in a factorial experiment design to facilitate the determination of the effect of stress range on specimen fatigue life. Maximum stress in all specimens was held constant at

75 percent of nominal yield for each steel type. Minimum stress during dynamic loading was determined by the maximum stress minus the stress range. All stress parameters were based on the tensile stress area or effective area of the threaded portion of the test specimens.

1.2.2 Factorial Design. Six series of specimens were fabricated for the study which included variations in steel type, diameter, thread type, and thread forming method. Two series supplied were also hot-dipped galvanized. A list of the test specimen series and their respective variables is given in Table 1.

The basic experiment performed for each test series was defined by the selected stress variable, stress range. Therefore, the influence of each variable could be evaluated at similar stress levels.

The basic factorial initially designed is given in Table 2. In this configuration, stress range was varied through three levels across all test series, providing two replicates in each cell. This design was used since it facilitated the systematic analysis of all test variables.

The loading system used for testing was capable of tension only loading, consequently the A36 steel specimens in the test series D, E, and F could not be tested at the maximum stress range of 30 ksi as shown in the initial design. These specimens were tested at stress ranges of 15 to 25 ksi to provide additional fatigue life data. Therefore, the basic experiment factorial was incomplete in that not all levels of stress range were tested for all series. Also, those specimens which did not fail and some which failed with sufficient threads remaining were retested. The replication in a cell of some test series was increased by using these specimens.

The final experimental design allowed the systematic evaluation of the effects of steel type for 1-3/8 in. diameter specimens at stress levels of 10 and 20 ksi for the combination of high and low strength steels. Also, the effect of bar diameter can be determined for the

A193 Gr. B7 steel at all stress ranges for 1-3/8 in. and 1-3/4 in. diameter specimens which have 8UN series cut threads.

In several cells, the final test factorial is confounded by differences in thread sizes. In a future study additional specimens of A36 1-3/8 in.-8UN and 2 in.-8UN cut threads will be tested to allow unconfounded statistical analysis of all test variables. The results of these tests will be presented in a subsequent report.

The final experimental design factorial for all specimen series and test variables are given in Table 3.

CHAPTER 2

TEST SPECIMENS AND EXPERIMENTAL PROCEDURE

2.1 Specimen Design

All anchor bolts in this study were 38 in. long with a 6 in. long threaded section in each end and were supplied with two nuts as shown in Fig. 1. These units were tested as shown in Fig. 2. This testing method provided a region of uniform uniaxial tension between the interior faces of the nuts.

2.2 Specimen Fabrication

All anchor bolts were fabricated from hot rolled bar stock cut to the specified length and threaded on each end with the appropriate thread series specified for each diameter and type of steel. In order to simulate as realistically as possible the quality of threads obtained in actual construction, all bolts and nuts were obtained through commercial vendors and suppliers. The nuts for all A193 and 4340 specimens were ASTM A194-73 heavy hex grade 2H nuts.

Although all uncoated threads were specified to conform to ANSI standards for a class 2A fit, undersized threads were measured on several test specimens. However, since anchor bolts with undersized threads may also be delivered to actual construction sites, these bolts were tested without special treatment. In addition, the nuts on all galvanized specimens were tapped oversize an unspecified amount to provide clearance on the galvnized external threads of the bolts. Although overtapping of galvanized nuts is standard practice, the ANSI standard does not apply to coated threads. Thread fit and its effect on anchor bolt fatigue life, along with the results of thread measurements are discussed in detail later in the interpretation of test results.

In order that material properties could be kept constant throughout each steel type tested, all anchor bolts of each steel and diameter were fabricated from bar stock from the same heat of steel. Two tension test specimens were machined from the quarter-diameter points from bar stock of each steel and diameter type according to the ASTM A370 standard for 0.5 in. diameter test specimens. The tests were conducted in a Tinius-Olsen 100-kip screw-type mechanical testing machine, and instantaneous results of load and elongation were plotted automatically. The testing speed was 0.025 in./min. until the static yield load was determined. The speed was then increased to 0.1 in./min. and maintained at that rate until the specimen ruptured. Elongation of all specimens were computed using an initial 2 in. gage length.

The average mechanical properties for each specimen type are given in Table 4. For comparison the mill test results which accompanied each steel type are also presented. The results of the laboratory tests are above minimum requirements for all specimens except Series F (A36, 2 in. stock). Measured dynamic yield for this series was only 74 percent of the specified 36 ksi minimum yield strength for A36 steel, while the mill report accompanying this purchase indicated the yield strength to be over 41 ksi.

Tests to determine chemical composition were conducted by an independent testing laboratory on each steel and diameter type. Samples were taken at random from previously tested fatigue specimens. The results of this analysis along with the mill report analysis and specification requirements are presented in Table 5. Both the laboratory analysis results and mill reports correlate well with the values and check variations allowed by the specifications for all except the Type F specimens. Laboratory results indicated the Type F steel had only 0.06 percent carbon, or about 1/4 of the normal percentage for A36 steel. Also the manganese content of the Type F steel was only 67 percent of the minimum required.

Both the mechanical tests and chemical analysis of the Type F steel gave results which showed this steel type to be understrength and out of specification. However, all other test series gave results that were within specification allowables.

Upon delivery to the laboratory, specimens were die marked on each end with a four character identifying code. Each specimen was coded by test series, stress range, replicate number and bar end. This specimen designation is given in Table 6 and Table 7 gives an index of test specimens by identifying code. Also, in order to randomize the effect of uncontrolled thread quality within a given test series, all specimens within a series were randomly marked for testing at the specified stress levels.

2.3 Loading Apparatus

The loading system was a 200 ton center hole hydraulic ram. A 50 cu. in. pulsator provided the loading. The pulsator uses a constant displacement, flow controlled, high-pressure hydraulic pump to maintain the specified maximum jack load. A variable-stroke hydraulic pump is used to vary the ram load by displacing a given amount of hydraulic fluid from the fully loaded system. The sinousoidal cyclic loading pattern is obtained by setting the stroke of the piston to the required displacement to allow the load in the ram to fall to the required minimum load. The piston then returns the displaced fluid to the ram to complete the loading cycle. Test frequency ranged from 400 to a maximum of 500 cycles per minute with most specimens being tested at the maximum frequency. Figure 3 shows a photograph of the complete loading system.

All specimens were tested in uniaxial tension with the load applied directly to the nuts by bearing plates which measured 8 in. X 6 in. X 1.5 in. thick. These plates were used to transfer the ram load directly to the inside face of the nuts as shown previously in Fig. 2. Three pairs of plates were utilized in order to accommodate each of the three different diameters tested. Machined aluminum spacers were attached to the bearing plates to provide an accurate means of radially centering the specimen in the loading ram. The accurate centering of the anchor bolt in the ram was done to ensure that the applied load was concentric with the bolt centerline. Small bending moments were measured in the bolts due to their initial out-of-straightness and the faces of the nuts not perpendicular to the axis of their threads.

2.4 Instrumentation

The test instrumentation consisted of a static strain indicator for measuring the output of strain gages applied to each specimen for the determination of bolt load and control of dynamic stress range. Two 0.64 in. gage length, 120 ohm, paper backed resistance strain gages were mounted longitudinally opposite each other at the middle of each specimen as shown in the photograph in Fig. 4. Two gages were used to compensate for any bending in the bar. During static loading, strain outputs were averaged and converted to give a nominal tensile stress. Typically, the difference between the two gage readings was less than 7 percent.

During the early stages of testing, dynamic stress range was set by displaying the strain output of a single gage on an oscilloscope which was calibrated to a known strain. Load range was increased until the desired strain range was displayed on the oscilloscope. Estimated accuracy of this system was considered to be ± 2 percent or the accuracy of reading the oscilloscope trace.

For later tests the strain gages were connected to an amplitude measuring module which contains a power supply for the strain gage bridge, a high gain amplifier, and a two stage voltage comparator. The comparator circuits compare the amplified strain signal with two calibrated DC voltages corresponding to the desired maximum and minimum strains. The difference between the desired strain gage output was displayed on an oscilloscope. This system enabled the desired dynamic load to be set within 1 percent.

Both static and dynamic loads as determined by the specimen strain gages were checked with a calibrated load cell placed in the loading system and were found to give values within 2 percent of the desired values.

2.5 Experimental Procedures

The sequence of testing was randomized within specimen series so that the effect of uncontrolled variables such as temperature or operator technique would also become random. As stated previously, the selection of test stress range for each specimen was also done randomly within each test series to randomize the effect of variable thread quality. By randomizing these uncontrolled variables, the effects of the variables could be considered as random error during the analysis of the test results.

All specimens were tested in the loading ram shown in Fig. 5. Each strain-gaged specimen was inserted through the ram and centered radially by the end bearing plates. The nuts were then placed on the ends of the bolt to complete the assembly. The exact position of the nut on the threaded portion of the bolt was not kept constant throughout the study, but was occasionally varied to prevent excessive wear on the loading ram, to insert a load cell, or to allow for retesting of failed specimens. The range of variation of nut position is given in in Fig. 6.

The assembled specimens were loaded statically to 75 percent of the minimum yield strength on the tensile stress area of the threaded bolt. Tensile stress area A_T as defined by ANSI is equal to:

$$A_T = 0.7854\left(D - \frac{0.9743}{n}\right)^2 \tag{1}$$

where D = the nominal bolt diameter and

n = the number of threads per in.

The desired stress level in the specimen was obtained by averaging the two strain gage readings from the gages placed at the center of the bolt. By averaging these readings, strains induced by seating moments were cancelled to give a net axial strain at the center of the bar. This strain reading at the gages was directly related to the stress on the tensile stress area by the following equation:

$$\epsilon_g = \frac{A_t \sigma_t}{A_g E} \tag{2}$$

where ϵ_g = the averaged strain reading from the gages

A_t = the tensile stress area

A_g = the area of the bolt computed from the average measured diameter at the gage location

E = the modulus of elasticity taken as 30000 ksi, and

σ_t = the desired stress on the tensile stress area

Each specimen was loaded statically in increments from zero to the maximum stress level at least three times before cyclic loading was begun. During these three loading cycles, strain readings which corresponded to maximum and minimum test stresses were recorded for each gage. The load in the bar as indicated by the strain gages was also checked by noting the total system pressure applied to the effective ram area, and bolt elongations at both maximum and minimum test stress levels were recorded with a 0.001 in. dial gage. These deflections were used to set the maximum deflection during dynamic loading, and the difference of these two readings was used to check the range of loading set by the strain gages during dynamic testing. Typically, the dial gage range could be read no closer than ±0.001 in. during the dynamic loading. However, this reading was usually within ±2 percent of the maximum static deflection.

After the static loading phase was completed, the load was again set to the maximum level and the pulsator system was engaged. The variable-stroke piston was manually adjusted to give the desired stress range as indicated by the strain output and test instrumentation readings as discussed previously. With the proper stress range indicated and checked by the dial gage deflection range, the maximum load level was adjusted to give the maximum dial gage deflection as recorded during the static loading stage.

From the final settings, the pulsator automatically maintained the mean load to within ± 2 kips. The effect of this mean load variation was most pronounced for the lowest load specimens, the 1-3/8 in. A36 specimens, where the load variation resulted in a maximum deviation of ± 5 percent of the mean load. However, the mean load was observed to remain essentially on the desired value, with only occasional slight deviations. Maximum deviation of mean load for the highest load specimens was approximately ± 1 percent.

Load range, as set by manual adjustment, remained essentially constant throughout the specimen life. However, slight variations up to ± 2 percent of the desired range were noted during testing and periodically adjusted to zero. These variations were attributed to the change in the pulsator hydraulic oil viscosity with fluctuations in ambient temperature and pulsator temperature.

2.6 Ultrasonic Inspection

Ultrasonic inspection of the specimen ends for crack initiation and propagation was used during load application for several specimens. However, since continuous observation was not possible, only intermittent readings were obtained. The inspecting unit used was an Automation Industries Model UJ portable ultrasonic reflectoscope equipped with a 0.25 in. diameter, 5MHz, longitudinal beam contact type transducer.

The ultrasonic inspection method uses high frequency sound waves which are transmitted through the material and reflected by cracks and other discontinuities in the sound path. These reflected signals are detected by the receiving unit, amplified, and displayed on an oscilloscope as a sharp vertical peak. The height of this peak is proportional to the reflected sound energy, and the horizontal position is proportional to the distance of sound travel.

The inspection method included two steps. First, the transducer was calibrated with a known reference flaw to give a vertical reference indication at 60 percent of the screen height. This calibration was taken vertically from an International Institute of Welding (IIW)-Type I standard ultrasonic reference block as shown in Fig. 7.[3] This nonstandard calibration was used for convenience rather than the standard horizontal orientation. Correlations of the sound level required at each calibration point to give the maximum flaw indication at 60 percent screen height showed that the horizontal calibration required a sound energy level of 10 decibels (db) greater than the vertical calibration position used in this study. The ultrasonic unit was also calibrated for distance on the same IIW-Type I calibration block. The photograph in Fig. 8 shows the inspecting unit and calibration block with the transducer positioned over the reference flaw for calibration.

The second step was to inspect each end for cracks as the specimen was being tested. The bolt ends were filed smooth to provide better sound coupling. Glycerol was initially used to couple the transducer to the specimen, but as the test progressed, a commercial couplant was found to be more satisfactory as no residue was left on the specimen after inspection.

The scanning level used was 30-35db above the reference flaw level. With this scanning level, thread profiles could normally be distinguished throughout the threaded portion of each specimen end as the transducer was moved around the bolt perimeter. This inspecting procedure is shown in the photograph in Fig. 9.

The data generated from the ultrasonic inspection of the bars was analyzed using the defect rating format used in the AWS Welding Code.[3] The flaws were indexed using the defect rating scale determined as:

$$D = a - b - c \tag{3}$$

where D = defect rating relative to a reflector at 1 in., db

a = db level of actual flaw to give 60 percent screen height indication

b = db level for reference flaw to give 60 percent screen height indication

c = attenuation correction for sound path length, db

The attenuation factor accounts for the increase in sound energy input required to maintain a constant flaw indication as the sound path distance increases. The AWS Welding Code determines the attenuation factor as

$$C = 2(t - 1) \tag{4}$$

where t = the distance of sound travel to flaw location, in.

This relation was checked experimentally using six calibration bars ranging from 1 to 6 in. in length and was found to give good correlation. Therefore, the defect rating scale allows the comparison of reflection indications relative to a known reference flaw (IIW-I) and common effective length.

In order to determine the size of detectable cracks, saw cuts were made in the threaded portion of a previously tested specimen to simulate cracks at different depths. Even though some of the notches were directly shadowed by larger, closer notches, all could be resolved for distance and approximate size of crack. Notch locations and dimensions along with the sound level defect rating for a 60 percent screen height indication are shown in Fig. 10.

CHAPTER 3

TEST RESULTS

3.1 Fatigue Test Results

The results of all fatigue tests are summarized in Table 8. The failure summary includes nominal stress range, maximum and minimum stress on the tensile stress area, and cycles to failure. Also included in this summary are the number of cycles and defect ratings of the first detected crack indication obtained from ultrasonic inspection of the end which failed. Since continuous inspection of test specimens was not provided, the first observed indication does not necessarily indicate time of initial crack formation or smallest crack detectable. Specimen designations which include an "R" indicate retests of unfailed specimens or retests of specimens that had failed with sufficient threads remaining to allow retesting.

Four specimens were originally tested to over 11 million cycles with no detectable crack indications from ultrasonic inspection and were subsequently removed from the testing apparatus. The four bolts included three Type E, 1-3/8 in.-8UN rolled A36, and one Type A, 1-3/8 in.-8UN A193, test specimens. The Type E bolts achieved over 16 million stress cycles at a stress range of 10 ksi with no ultrasonic crack indications. The other Type E specimen was tested at a stress range of 15 ksi and also showed no crack indications after 11 million cycles. The Type A specimen was tested at a stress range of 10 ksi to 11 million cycles with no cracking. All other high strength specimens failed between 1.4 and 2.7 million cycles at this stress range.

The three Type E specimens which did not fail were retested at a higher stress range of 25 ksi to obtain more failure points. One other Type E bolt was retested at the initial stress range of 20 ksi. Two Type D specimens, 1-3/8 in.-6UNC cut A36, were also retested at 25 ksi for a total of six retested specimens. It should be noted that bolts which failed in the first test also failed on the same end in the retests.

3.1.1 Crack Initiation and Growth. Due to the inherent nature of nut and bolt loading configurations, visual inspection for fatigue cracks was impossible during uninterrupted testing. However, ultrasonic inspection was used during load application and proved quite reliable in determining crack locations and in estimating cracked area. Crack indications during testing were obtained for 16 of the total 42 individual tests performed. From this data, the crack causing failure was seen to initiate at the first fully engaged thread from the loaded face of the nut in all but one series tested. In five of six first D series specimens (1-3/8 in., A36, UNC, galvanized), ultrasonic inspection indicated initial crack initiation beginning at approximately two-thirds of the nut length from the loaded face of the nut. However, retest of two of these D series specimens resulted in cracks initiating from the first fully engaged thread as the majority of all other specimens inspected had performed.

The photograph in Fig. 11 shows characteristic failure surfaces and corresponding points of initiation for all specimen types. All specimens in this photograph illustrate the first engaged thread as the point of initiation and subsequent single failure surface as observed in all except the Type D specimens. The photograph in Fig. 12 shows cross sections of two different D series failed ends. Although the failure surfaces are at or near the first engaged thread of the nut, multiple cracks can be observed within the nut length. These cracks are the initial cracks detected by ultrasonic inspection during cyclic loading.

After initiation, crack growth was observed to follow two basic stages of propagation. Following initiation, cracks first progressed toward the center of the cross section along a straight-line front, perpendicular to the radial line from the point of initiation.

The second stage of crack growth was characterized by the development of the straight-line crack front into a crescent line. Crack propagation was observed to progress circumfrentially as well as radially inward. This cracking pattern continued until failure occurred. The photograph in Fig. 13 shows both stages of crack growth leading to fracture for Ends A and B of a single specimen. The right side of the figure shows the fatigue failed end at fracture with the characteristic crescent surface of second stage fatigue cracking. The left side of the figure shows the extent of first stage cracking, which was revealed by the static pull-out test, that developed in the unfailed end in the same number of cycles that caused failure of the opposite end of the specimen. The difference in fatigue behavior between the two ends as shown above indicates the amount of scatter that can result even when testing identical specimen ends under identical applications of load.

Post-ultrasonic inspection of all tested specimens showed that 58 percent of the unfailed ends showed ultrasonic crack indications. However, Table 9 shows a wide variation in unfailed end crack behavior as a function of specimen type. The fact that no crack indications were observed at the unfailed end of any Type E specimens also indicates the wide range of variability which can accompany the initiation stage of crack growth.

3.1.2 Analysis of Variance. The effects of the controlled variables were systematically evaluated using the statistical technique of analysis of variance. Regression analysis was also used as an additional quantitative check for variable effects. In both statistical evaluations performed on the test data, the observed fatigue lives were transformed to the logarithm (base 10) of fatigue life cycles.

Analysis of variance can be used to analyze test results for combinations of independent variables and their corresponding significance on the outcome of the results. By analyzing only two variables at a time, each variable may be tested independently of the other for significance, and the degree of their interaction which may also be significant will be minimized.

The test for significance checks the hypothesis that each observation comes from a normal distribution and that there is no difference in the means of subgroups due to the independent variable. The statistic used to test this hypothesis is the F ratio. This ratio is the mean sum of squares for the individual treatment divided by the residual sum of the squares for all observations. These calculated F ratios are compared to tabulated F ratios to determine significance. If the calculated value of F is greater than the tabulated value, the hypothesis is rejected and the variable is said to be significant. Conversely, if the calculated F ratio falls below the tabulated value, the hypothesis is accepted that no significant effect exists.[4]

The tabulated value of F depends on the number of variable levels and sample size, and also on the probability of erroneously concluding that there is a significant difference when there actually is none. This error is defined as an error of the first kind and is denoted by α. An error may also be made by failing to find a difference that really exists, thus committing an error of the second kind denoted by β. The probability β depends on the magnitude of the difference, sample size, and the level of α selected for the test.[9]

The choice of α is completely arbitrary. However, as α increases, β decreases. A significant level of $\alpha = 0.01$ or 0.05 is typically used for experimental analysis where the mean difference must be very large before the variable effect is considered to be significant. For this experiment α was chosen to be 0.05 since the intent of this study is to determine which variables have the largest effect on specimen cycle life.

Seven different factorials, Figs. 14 through 17, were used in the analysis of variance to test for variable significance. Of these complete groups of observations, only two factorials have exactly two variables of classification. As shown in Figs. 15 and 16, respectively, Factorial II for the effect of diameter and Factorial IV for the effect of steel type have only two variables, whereas all other factorials analyzed are confounded by the difference of thread series within factorial groups. This difference must be considered when interpreting results for variable effects. Additional tests are planned that will remove this third variable and allow unconfounded analysis with only two variables. These additional results will follow in a subsequent report.

All analysis of variance results are summarized in Tables 10 through 13. In all cases, stress range was used as one of the two variables of classification. The other variables considered were thread forming method, diameter, and type of steel.

3.1.2.1 Effect of Thread Forming Method. The variance of the fatigue life due to different thread forming methods was investigated by examining the results of Factorial I which are summarized in Table 10. The results show that stress range is the significant variable and that insignificant interaction exists. Although the second variable, forming method, is confounded by differences in thread series, the total effect is seen to be insignificant on the specimen cycle lives.

3.1.2.2 Effect of Diameter. The variance due to difference in bar diameter was investigated using Factorials II and III. The results are summarized in Table 11. Factorial II results indicate no significant difference for bar diameter and no appreciable interaction between stress range and diameter. Stress range is the dominate variable and accounts for almost all the specimen variation.

The results of the Factorial III analysis show F ratios very much greater than tabulated values for both stress range and the second variable, bar diameter. However, the interaction of these variables is seen to be insignificant, indicating that stress range is significant independently of all other variable effects. Although bar diameter is indicated to be significant, the variance cannot be attributed only to diameter difference since the factorial is confounded by thread series differences and steel strength differences as indicated in Table 4 of mechanical properties of A36 steel.

3.1.2.3 Effects of Steel Type. The analysis to determine the effects of steel type was performed on Factorials IV through VII. The results are summarized in Tables 12 and 13. Factorial IV compares A193 and 4340 steels and the results indicate no significant difference existed between these two high strength steels. Again, stress range was highly significant with no significant interaction at the 5 percent level. Factorials V, VI, and VII which compared high strength steels to A36 steel, also showed significant effects for the stress variable with little interaction with other variables at stress ranges of 10 and 20 ksi.

However, Factorials V, VI, and VII all indicated a significant difference in behavior between high strength and A36 steel. The comparison of fatigue lives indicates that the specimens from A36 steel do exhibit longer lives than comparable high strength specimens of A193 or 4340 steels under the same conditions of stress. By examining the results of Factorials V and VI, the confounding effect of either thread series or forming method is seen to produce approximately the same order of results. Therefore, the effect of steel type between high and low strength steel can be considered significant over either thread size or forming method.

3.1.2.4 Effect of Stress Variable. The results of all variance analyses of Factorials I through VII have indicated that stress range is the dominate variable regardless of other variable effects. By examining the summaries of results tabulated in Tables 10 through 13, it can be seen that this variable is also free from interaction with other variables.

3.1.3 Regression Analysis. The experimentally derived S-N (stress-life) curve may be described mathematically by regression analysis. The method of least squares is used to fit the finite life portion of the data to the equation:

$$Y = B_1 + B_2X \tag{5}$$

To linearize the stress-fatigue life relation, transforms for both Y and X must be used. From Reemsnyder[12] both semilogarithmic and logarithmic transforms will linearize the S-N curve for fatigue data. The semilogarithmic Model A and logarithmic Model B may be written as:

$$\text{Model A:} \quad Log_{10}N = B_1 + B_2S \tag{6}$$

$$\text{Model B:} \quad Log_{10}N = B_1 + B_2Log_{10}S \tag{7}$$

where N = the finite cycle life

S = stress variable

B_1, B_2 = constants which are determined by the least squares analysis of the data

The stress variable used in the regression analysis of all test results was the main experimental variable, stress range.

The regression analysis allows the effect of stress variables to be determined outside the range of factorials investigated by analysis of variance and also to verify the significance or insignificance of the effects reported in the analysis of variance.

Confidence intervals for the regression lines may also be determined from the standard error of estimate and sample size for any desired percent survival and confidence level. These lower bounds may be helpful in determining design criterion from limited sample size fatigue tests. The confidence interval s for all regression analysis was chosen as the 95 percent confidence level for 95 percent survivals or failures and is indicated by a dashed line banding the mean regression line from the test data.

The results of all regression analysis are summarized in Tables 14 through 16. These results indicate that the best fit of the data, in terms of largest correlation coefficient and smallest standard error of estimate, is most often provided by the log-log model. Therefore, this model was chosen to represent the results graphically in Figs. 18 through 24.

Figure 18 shows the individual mean regression lines for all high strength test specimens, Series A, B, and C. It is apparent from Fig. 18 that no significant difference existed among specimen Types A, B, or C. This observation verifies the results of the analysis of variance for Factorials II and IV, that all high strength specimens behaved similarly regardless of diameter or type of steel. The mean regression line for all high strength specimens shown along with the actual test data in Fig. 19 indicates that the specimens all behaved similarly.

The mean regression lines for the 1-3/8 in. diameter high strength steels and the A36 steel specimens in Fig. 20 indicate a significant difference between the fatigue life of the 1-3/8 in. A36 specimens and the higher strength steels. The higher strength steels yielded smaller fatigue lives at all stress ranges tested. This difference in behavior was also noted in the analysis of Factorials V, VI, and VII.

The fatigue results and mean regression lines of all the A36 steel specimens are shown in Fig. 21. The 1-3/8 in. A36 steel specimens with rolled and cut threads yielded comparable fatigue lives. The 2 in. diameter A36 steel Type F specimens produced shorter fatigue lives than the 1-3/8 in. A36 specimens. This difference, also noted in the analysis of variance for Factorial III, cannot be attributed to differences in diameter alone, since the total difference is compounded by understrength steel as noted in the mechanical properties listed in Table 4, and gross differences in thread sizes. Figure 22 shows the relationship of the high strength steels to the A36 specimens, with the intermediate results of the Type F specimens clearly evident.

The mean regression lines for specimen Types D and E, 1-3/8 in. A36, as shown in Fig. 23 can be used to indicate that no significant difference in fatigue life resulted from differences in thread size of thread forming method. Although the two types of specimens behaved similarly with respect to fatigue life in the finite life region, crack initiation and growth characteristics were quite different as discussed previously. Multiple cracking which initiated deep in the nut was observed in the cut thread series while single crack initiation and growth was observed for the rolled thread specimens. Also, all Type D (cut threads) specimens achieved failure, whereas Type E (rolled thread) specimens were tested to the same number of cycles with no indications of cracks at stress ranges of 15 and 10 ksi.

The mean regression lines and 95 percent confidence intervals for both high and low strength steels are given in Fig. 24. This plot indicates that A36 steel gives significantly longer lives at all levels of stress range than the high strength steels. However, due to the large amount of scatter in the A36 test results, the lower bound 95 percent confidence lines for 95 percent survivals for both high and low strength steels are seen almost to coincide. Also, the entire confidence interval for the high strength steels is shown to lie entirely between the mean regression line and lower 95 percent confidence line for the A36 steel.

To insure the validity of both the analysis of variance and the confidence intervals from the regression analysis, three requirements must be met:[12]

(1) The test must give unbiased results

(2) The transformed lives $Log_{10}N$ must be normally distributed

(3) The transformed lives, $Log_{10}N$ must have a common standard deviation as estimated by the standard of estimate

The first requirement was satisfied by the experimental design. For the verification of the second and third requirements, the method of order statistics was utilized.[11,12] Cumulative frequency diagrams were constructed for high and low strength steels for each level of stress range. The steels were grouped in this manner, since both statistical tests indicated a significant difference between the high strength and A36 steel in both estimations of mean fatigue life and standard error of estimate.

The plotting position P was assigned to each data point by the relation:[11]

$$P_i = \frac{i - 3/8}{N + 1/4} \tag{8}$$

where i = the position number

N = the population size.

The results are plotted in Figs. 25 and 26. The mean fatigue life was estimated for each level of stress range by the logarithmic Model B and plotted at the 50 percent survival level. The standard error of estimate was used to determine the slope of the cumulative frequency line through the estimated mean life. It may be seen that the transformed observed cycle lives fit the predicted cumulative frequency diagrams reasonably well for all stress levels for both high strength and A36 steel. Therefore, the second and third requirements have indeed been met and all statistical assumptions are validated both for the analysis of variance and regression analysis.

3.1.4 Summary of Fatigue Test Findings. Findings of all analysis of the fatigue test results can be summarized as follows:

(1) Stress range was the most significant variable influencing cycle life.

(2) Differences in the behavior of A193 Gr. B7 steel and heat treated 4340 steel were insignificant.

(3) Differences in diameter for A193 Gr. B7 steel had an insignificant effect on cycle life.

(4) The failure lives of A36 steel were significantly larger than exhibited by the higher strength steels.

(5) Thread forming method had no apparent effect on cycle life.

(6) The crack causing failure initiated at the first fully engaged thread in all specimens except Type D.

(7) Type D specimens exhibited multiple cracking with the first crack initiating inside the nut, approximately two-thirds of the nut length inward from the loaded face of the nut.

(8) The rolled thread specimens exhibited no fatigue cracking at the 10 and 15 ksi stress ranges.

(9) The log-log model relating stress range to cycle life was seen to give the best fit to the S-N relationship

(10) Type F specimens gave intermediate results between all other A36 specimens and the high strength bolts.

(11) High strength and low strength steels were banded in to separate S-N curves and both showed to be log normal.

3.2 Full-size Tension Test Results

Tension tests to failure were conducted for all six bolt types tested in this investigation using specimens fabricated in the same lots as those used in the fatigue tests. These tests were done in the same loading ram and end fixtures used for the fatigue tests. A pressure transducer calibrated in the loading ram with a calibrated load cell was used to measure ram load. Displacement relative to the loaded face of the nuts was measured using both a 0.001 in. dial gage and a linear voltage displacement transformer. With this instrumentation, digital readings for load and displacement were obtained as well as a simultaneous plot of load versus displacement. The loading system is shown in the photograph in Fig. 27.

On all specimens except the 1-3/8 in. A36, Types D and E, a 10 in. gage length was marked in the unthreaded portion of the specimen to determine the percent elongation caused by yielding of the bolt shank. Gage length within the threaded regions was left unmarked due to the problem of defining percent elongation in this region. All specimens except the Type B specimen had an initial distance between the bearing faces of the nuts of approximately 34 in. This distance in the Type B bolt was decreased to 30 in. since the bolt had been previously tested in fatigue and the fatigue failure surface had to be removed to accommodate a new nut.

In an attempt to quantify thread stiffness, 0.0001-in. dial gages were mounted as shown in Fig. 28 on the ends of the bolts to measure displacement of the bolt relative to the nut as the specimen was loaded elastically. These measurements were taken as an indicator of thread stiffness to be later correlated to the relative thread fit. However, this method proved unsuccessful in determining any meaningful correlation of thread stiffness to thread fit due to a large amount of scatter in the data.

Plots of load versus displacement of the full size tension specimens are shown in Figs. 29 through 34. Static loading was used for all specimens until indications of first yield were observed. Then the loading was applied dynamically at a ram extension rate of approximately 1 in. per minute within the 34 in. gage length. Plots which were recorded automatically show vertical lines in the region where load was applied dynamically. The displacement of the specimen was held at these points for two minutes. The drop in load indicated is a consequence of the strain rate effect on the mechanical behavior of the specimen. The load at the end of this time period was considered to be the static behavior of the specimen. Figures 32 and 33 were not recorded automatically and indicate static loading for all values past the elastic region. Calculated yield and ultimate loads taken as the measured dynamic yield and ultimate stress from Table 4 applied to the tensile stress area also are shown on each plot.

All specimens failed in the threaded portion of the bolt between the nut and the smooth shank. Specimen Type E with rolled threads failed near the first thread formed by the rolling process as shown in the photograph in Fig. 35. All other specimens failed well within the threaded region.

The A36 bolts exhibited good ductility with failure elongations ranging from 30 to 50 times the displacement at first yield. Less ductility was observed with the high strength bolts where ultimate displacements were only three to seven times the elastic displacement.

In all specimens, most elongation was confined to the threaded portion as indicated by the small percent elongation of all 10 in. gage lengths marked. The photograph in Fig. 35 shows the gross yielding and necking of the threaded portion which preceded the failure of the 1-3/8 in. A36 specimens. Overall elongations indicated on the plots of Figs. 29 through 34 were considerably smaller than those determined in Table 4 of mechanical properties due to the difference in cross section sizes within the specimen length.

Measured ultimate loads for all A36 specimens exceeded the calculated ultimate load from 2 to 44 percent. However, the ultimate loads of Types A and C of the high strength steels were from 3 to 4 percent lower than the calculated ultimate using the tensile stress area. Ultimate strengths were compared in the high strength steels due to the problem of satisfactorily defining a gage length which can be used to determine the 0.2 percent offset yield strength.

Generally, all test specimens performed satisfactorily in the full-size static tension test. Although some of the high strength specimens gave slightly lower ultimate strengths than the calculated capacity, all results indicate adequate performance for all specimens when considering most design calculations to be based on minimum nominal yield and ultimate strengths.

It should be noted that the Type B specimen, 1-3/4 in. A193, had previously been tested to failure under fatigue loading. Although ultrasonic inspection of the unfailed end indicated no cracking initiated by the fatigue loading prior to the load test to ultimate, a first stage fatigue crack approximately 0.16 in. deep and 0.87 in.

along the chord, did exist and triggered a brittle fracture failure during the tension test. This crack is pointed out in the photograph in Fig. 13. Although this failure occurred well above the calculated yield load and even above the calculated ultimate load, very little plastic deformation and very little warning of impending failure was observed in this test as shown in the plot of Fig. 30.

It was also observed that deformations within all the nuts remained essentially elastic in that all nuts could be removed by hand following testing. However, none of the nuts could be advanced farther on the bolt due to the deformation of the threaded portion of the bolt within the tested region. The deformations in the nut remained elastic most likely because of the complex state of stress in the nut which tends to elevate the yield point and suppress yielding.

3.3 Charpy Impact Testing Results

Standard Charpy V-notch Type A impact specimens were machined and tested in accord with ASTM E23-72 for all types of steel at each diameter investigated in this study. All specimens were tested in a Tinius Olsen impact testing machine. The machine calibration was checked using Army Materials and Mechanics Research Center specimens tested at $-40^{\circ}F$, and was found to be within allowed tolerances. Specimens were machined from the anchor bolt quarter points in the longitudinal rolling direction and the notches were placed on the side closest to the original bolt periphery.

For test temperatures between -90° and $+40^{\circ}F$, specimens were submerged in a mixture of methyl alcohol and dry ice as shown in the photograph in Fig. 36. Specimens were immersed in liquid nitrogen (N_2)for testing at $-320^{\circ}F$. Elevated temperatures between 100° and $160^{\circ}F$ were obtained by submerging the specimens in a constant temperature water bath, maintained with a portable electric heating element. Thermometers were used to monitor all temperatures between -90° and $+160^{\circ}F$ and an electric stirrer was used in both high and low temperature baths to minimize any temperature gradients. All temperatures recorded were accurate to within $\pm 1^{o}F$.

Plots of Charpy impact energy (ft-lb) versus temperature (^{o}F) for the two diameters of A193 steel and the heat treated steel, and the two diameters of A36 steel are shown in Figs. 37 and 38, respectively. Figure 37 shows the Charpy upper shelf beginning approximately at $0^{o}F$ for both series of A193 steel at an energy level of 60-70 ft-lbs. The 4340 steel behaved similarly having an upper shelf to transition intersection at $0^{o}F$ at an energy level of 45 ft-lbs. Both of these high strength steels showed a gradual energy transition.

Both diameters of A36 steel showed a steep transition within the service temperature range as shown in Fig. 38. Also, the Type F specimens, machined from the 2 in. diameter A36 steel, absorbed energies up to 200 ft-lbs at temperatures of 120^{o}-$150^{o}F$ without complete fracture indicating very good toughness at temperatures over $100^{o}F$ for this steel.

The results of these Charpy V-notch tests were evaluated using AASHTO material toughness specifications[1] and PVRC recommendations on toughness requirements for high strength bolting materials.[10] Both specify a minimum Charpy V-notch (CVN) impact value for the lowest expected service temperature.

The AASHTO specifications are based on a 15 ft-lb CVN impact value which must be met at the test temperature specified for three regions of anticipated lowest service temperature. These groups are defined as follows:

Group 1: Minimum service temperature $0^{o}F$ and above
Group 2: Minimum service temperature -1^{o} to $-30^{o}F$
Group 3: Minimum service temperature -31^{o} to $-60^{o}F$

The test temperatures for these service groups are determined by applying a strain-rate temperature shift between the test temperature and lowest expected service temperature. This temperature shift takes into account the fact that the toughness of structural steels decreases as the loading rate increases. Since the CVN impact test is a dynamic test, results must be modified to account for an actual structural loading rate which is normally intermediate of static and dynamic test rates. The magnitude of this shift has been correlated to the room temperature yield strength of steels, being largest for low strength steels and decreasing to zero for steels with yield strengths greater than 140 ksi.

The basic 15 ft-lb toughness level mentioned above may also be modified using fracture mechanics concepts to account for increases in yield strength. An increase in yield strength is normally accompanied by an increase in allowable stress so that a corresponding increase in CVN energy is required to assure the same level of flaw tolerance.

Required test temperatures and CVN energies for each AASHTO regional group are presented for A193 and A36 steel in Figs. 37 and 38, respectively. AASHTO specifications for A514 steels were used for the A193 Gr. B7 test specimens since both have approximately the same nominal yield strength. Also, it should be noted that no current provisions are made in the AASHTO specifications for the heat treated 4340 steel.

Figure 38 also shows the AASHTO requirements for all three service regions for the A36 steel. It can be seen that specimens from both diameters greatly exceed the requirements of Group I and that both also meet the toughness requirements of Group II. Although the Type F specimens did not pass the requirements of Group III, both steel types exhibit excellent toughness for general highway applications. This observation is reinforced by the fact that all A36 fatigue test specimens failed by net section yield at a maximum stress level of 0.75 percent of nominal yield strength.

Figure 37 shows the 25 ft-lb AASHTO CVN energy requirement for all three service regions for the A193 steel. Again, it can be seen that these toughness requirements are easily met. This observation is reinforced by the fact that specimens from both diameters of A193 steel exhibited sufficient toughness to cause net section yielding to control all fatigue test failures of this steel type.

The PVRC toughness recommendations for bolting steels are also based on fracture mechanics concepts and are applicable to steels having yield strengths in excess of 100 ksi. For bolt diameters below 1 in. no test is required. However, for diameters over 1 in. to 3 in. a 35 ft-lb CVN energy level is recommended. This requirement applies at the lowest service temperature of the structure. This level is indicated on the plot of Fig. 37.

It can be seen that CVN energy levels for both diameters of A193 steel exceed this level of toughness by a factor of two for both AASHTO Groups 1 and 2 and do not fall below the PVRC 35 ft-lb level until temperatures below $-90^{\circ}F$ are reached. However, the 4340 steel is seen to fall below the PVRC requirement at a temperature of only $-20^{\circ}F$. Since the 4340 steel has a yield strength above 140 ksi, there is no temperature shift between static and dynamic loading rates and the test temperature indicates actual service toughness levels.

Although the 4340 steel tested in this project meets the minimum PVRC toughness requirements down to $-20^{\circ}F$ some highway structures may require lower service temperatures and a corresponding increase in toughness to insure against brittle fracture under high service stresses. Since there is no guarantee that other heats of 4340 steel will not have a higher transition temperature range than the steel used in this experiment, CVN impact tests should be specified to insure sufficient toughness levels.

3.4 Ultrasonic Inspection Results

Ultrasonic crack growth data, summarized in Table 17, was obtained for 16 specimens during the fatigue testing. All specimens showed an increase in reflected sound level with increasing stress cycles. This increase can be related to an increase in reflector (crack) size or crack opening with time.

Although this trend was observed for all specimens the rate of increase was observed to vary considerably from specimen to specimen as shown graphically in Fig. 39 where defect ratings (from Eq. 3) are plotted against percent of specimen cycle life. Although data points from only two specimens have been connected for clarity, data points are given for all readings and are classified into three basic groups:

(1) Basic specimen data

(2) Multiple crack specimen data

(3) Bending and elevated temperature data

The basic specimen data includes readings from all specimen types except Type C and represent a wide range of growth rates as indicated by the difference in the two sets of connected data points. The scatter in the basic data was completely random and independent of any differences in steel, diameter, test stress range, or sound path distance.

Multiple crack specimens are grouped in the lower portion of the graph and indicate readings from Type D specimens which showed cracks forming well inside the nut as previously reported in the fatigue test results. Although these cracks formed first, they were not the final failure crack and were not included in the basic test data group which indicates cracks at the first engaged thread. However, limited data on the growth rate of the failure crack at the first engaged thread of two Type D specimens fell directly in line with the data of the basic specimen group.

As indicated in this same figure, one specimen was subjected to considerable bending and elevated temperature during fatigue testing. Strain gage readings indicated over 13 percent bending, and ram temperature was measured at approximately 150°F during the testing of this specimen. It is hypothesized that these two conditions may have contributed to the significantly greater rate of crack propagation in this specimen as shown by the data points in the upper right corner of Fig. 39. Also, inspection of this specimen was hampered by the elevated temperature which caused difficulty in effectively coupling the transducer to the specimen end.

Figure 39 also shows a wide range in defect rating for the completely failed end at 100 percent of observed cycle life. This variance can be attributed to such differences as slightly curved failure surfaces, failure surface texture, poor sound coupling, and operator techniques and judgment.

If both the multiple crack data and the bending and elevated temperature data are considered to be exceptional cases of the basic specimen ultrasonic inspection results, arbitrary boundaries representing minimum and maximum percent cycle life consumed may be drawn as a linear function of defect rating as shown in Fig. 39. Although this arbitrarily drawn band represents a scatter of over 40 percent of total specimen cycle life for a given defect rating, these lines may be used for selecting scanning levels and intervals for ultrasonic inspection programs. The following example will be used to illustrate the procedure for implementing an inspection program from the above cycle life boundaries.

Consider an anchor bolt that has been in service for 10 years with the nut face 4 in. from the end of the bolt and a reference flaw calibration of 6db. In order to insure that no less than 40 percent of the fatigue life has been used, the scanning level would be determined using the lower bound minimum cycle life defect rating for 40 percent lift and Eq. 3 as follows:

$$D = a - b - c$$

$$23\text{db} = a - 6\text{db} - 6\text{db}$$

$$a = 35\text{db}$$

where D = 23db (from minimum cycle life consumed, Fig. 39)

b = reference flaw calibration level

c = attenuation factor from Eq. 4

a = absolute scanning level

If at a scanning level of 35 db no crack indications are seen the maximum percentage fatigue life consumed up to the time of inspection would be 40 percent. The corresponding minimum percentage fatigue life remaining would be 60 percent. The minimum fatigue life of the bolt in years is the service life in years at the time of inspection divided by the maximum fraction of fatigue life consumed. In the example this would be 10 years divided by 0.4 or 25 years. The next inspection should be performed in the

$$\frac{(100\% - 40\%) \times 10 \text{ years}}{40\% \times \text{F.S.}} \tag{9}$$

years or in the next 7.5 years in order to find a crack before complete fracture using a factor of safety (F.S.) of 2.

If the same scanning level is used for the next inspection and again no crack indications are found, the 40 percent life now becomes 17.5 years (10 years + 7.5 years) and the next inspection interval becomes

$$\frac{(100\% - 40\%)\ 17.5 \text{ years}}{40\% \times 2} = 13.1 \text{ years} \tag{10}$$

It should be noted that as inspections are performed and no crack indications are found, the inspection interval increases. However, changes in loading or safety requirements between inspecting intervals should be considered and inspection frequency altered accordingly.

Correspondingly, if the initial inspection at a scanning level of 35db resulted in a crack indication with a defect rating of 32db, the upper bound maximum consumed cycle life curve must be entered to find the minimum life remaining and next inspection interval. Figure 39 shows that a defect rating of 32db corresponds to a maximum of 60 percent cycle life consumed. The corresponding minimum fatigue life for the example would be 10 years divided by

0.6 or 16.7 years. Therefore, using the format of Eq. 9, the next inspection interval must be no greater than

$$\frac{(100\% - 60\%)}{60\%} \times \frac{10 \text{ years}}{2} = 3.3 \text{ years} \tag{11}$$

If the next inspection shows additional crack growth, the inspection interval will need to be reduced. If no growth is seen in the second inspection, the interval may be increased by substituting the total service life at the time of the inspection into Eq. 11. However, if the defect rating falls below 15db, immediate action should be taken to prevent a catastrophic failure. Although as much as 40 percent of the cycle life may be remaining, not enough data is available to determine what percentage of life is actually left.

Caution should also be given against the direct use of Fig. 39 for determining maximum and minimum percent cycle life from the values of defect rating shown in this figure. The values of defect rating used in this figure were generated using a reference flaw calibration of 6db taken from the vertical position as shown in Fig. 7. If any other distance or flaw is used as a reference, the absolute values of defect rating and scanning level will need to be modified accordingly. For example, if a horizontal reference flaw orientation is used to establish the reference flaw calibration level b, 10db should be subtracted from the ordinate of Fig. 39.

In general, ultrasonics were found to be quite reliable in locating flaws and characterizing them with respect to a relative reference when specimens were carefully inspected. However, a flaw that had previously been identified during fatigue testing remained undected after a quick inspection prior to use in the full-size tension tests. The crack was approximately the same size and shape as the Type B simulated saw-notched specimen discussed previously and shown in Fig. 8.

Although the flaw was missed in a quick inspection, it should be noted that this size flaw was detectable when the inspection was carefully performed. This fact emphasizes the need for carefully structured inspections which should be unrushed and conducted by skilled technicians. In addition, careful records should be kept which include the operator's name, equipment used, calibration settings, inspection results, and any unusual circumstances surrounding the inspection of each bolt since inspection may have time intervals of several years.

CHAPTER 4

INTERPRETATION OF FATIGUE TEST RESULTS

4.1 Effect of Thread Fit

For all specimens tested there was an equal probability for failure to occur at either end of the bolt with respect to all five basic test variables. Loading was the same at each end of the ram, and diameter, steel, thread series, and thread forming methods were constant for each specimen. In a sense, each anchor bolt was like two individual specimens, where only one end would reach complete fracture while the other end was still capable of sustaining the maximum load. Since 42 percent of all unfailed bolt ends indicated no signs of cracking when inspected ultrasonically, some difference must exist between the failed and unfailed anchor bolt ends that accounts for the variance in fatigue life behavior. Although the difference may be due only to experimental scatter, spot checks of thread dimensions which were made upon delivery of the test specimens indicated considerable variations in thread diameter within test series groups that may be partly responsible for these differences in fatigue life.

Since experimental control of thread details were specified only to be within ANSI Class 2A tolerances,[2] actual thread fit was not within the scope of controlled variables of this study and was considered as a random variable when statistical analyses were performed on the test results. In an attempt to correlate any subtle differences in the thread fit with the specimen's fatigue behavior, thread measurements were taken from both the failed and unfailed specimen ends after all testing was completed. Along each bolt end three measurements of major diameter and pitch diameter were taken in the undamaged threads as close to the failure surface as possible. The nut was also removed whenever possible and its minor diameter measured. Figure 40 defines these three thread diameter dimensions with respect to the specimen cross section.

Comparisons of the measured major diameters and pitch diameters indicated that either measurement could be used to characterize the dimensions of the thread profile. Since the major diameter is an easier dimension to measure, all correlations of bolt dimensions to specimen fatigue behavior were investigated using major diameter measurements.

Frequency diagrams showing the distribution of these major diameter measurements for the high and low strength steel specimens are given in Figs. 41 and 42, respectively. Nut minor diameter measurements for all specimen types are shown in the frequency diagrams of Fig. 43. In all three figures, the average of all readings for each type of specimen are indicated. The maximum and minimum tolerances shown on these diagrams are for ANSI B1.1 Classes 2A and 2B (external and internal threads, respectively) thread fits and apply only to uncoated threads. The minimum major diameter tolerance shown applies to unfinished hot rolled bars. Since all specimens were fabricated from hot rolled stock, this minimum tolerance which is 0.008 to 0.011 in. less than that allowed for finished bolts may be applied. Also, coated external threads, specimen Types D and F, by ANSI Standard B1.1 are not to exceed the nominal bolt diameter after coating. In addition, the tolerances shown for coated nuts, Types D and F, are for reference purposes only since ANSI Standard B1.1 does not specify tolerances for coated nuts.

Comparisons of measurements for all uncoated bolts show a wide variation between tolerance bounds in all series, but only Type B (1-3/4 in., 8UN) threads show the average of all failed end measurements to fall below the minimum major diameter tolerance. Coated specimens also showed a variation in measurements. Although only one measurement of the Type D galvanized specimens exceeded the nominal diameter limit, all of the 2 in. Type F specimens were over the nominal diameter maximum by an average of 0.007 in. due to the galvanizing.

Comparisons of nut minor diameter measurements for all specimens show a relatively small variation in all nut diameters for all except the Type B nuts where the range of readings was 0.032 in. as compared to 0.008 to 0.02 in. for all other specimen types. Of the uncoated specimen types (A, B, C, and E), Types A and C were entirely within tolerances, while Type B showed wide variations both above and below tolerances, and Type E averaged 0.004 in. over the maximum tolerance. Although the nuts for the Type E rolled specimens were measured to be slightly oversized, hand tightening indicated a smooth, snug fit. However, the combinations of oversized nuts and undersized bolts could be felt in the hand tightening of the Type B specimens where considerable play in the threads could be felt. Also, the threads appeared ragged with a very rough surface finish.

With respect to specimen fatigue life, 63 percent of all specimens failed on the end with the smaller average major diameter. When neglecting the cases where the difference between the average major diameter of the two ends of the specimen was less than the average standard deviation of 0.005 in. for all thread measurements, 10 of 14 cases (71 percent) failed on the end with the smaller average major diameter. Although these observations tend to indicate a trend for specimen failures, there was insufficient control of the nut and bolt dimensions and too much missing data in the actual thread measurements to draw any conclusions from this data.

Comparisons of observed fatigue life with absolute values of average thread major diameter showed no apparent correlation or adverse effects on fatigue life for specimens which were slightly undersized. For example, the average major diameter of specimen end B22B was 1.718 in. or 0.007 in. undersized and gave a fatigue life of 181,000 cycles before fracture, while specimen B21A which was tested at the same stress range failed at 138,810 cycles and had an average major diameter on the failed end that was 0.007 in. over the minimum tolerance. In another case, specimen end BDOT's average major diameter was 1.706 in., 0.019 in. below the minimum specified major diameter and gave a fatigue life of 2,031,000 cycles at a stress range of 10ksi. Its counterpart, Specimen B11A was over the minimum tolerance by 0.004 in. and endured only 1,402,700 cycles before failure even though it was tested at the same nominal stress range of 10 ksi. This data indicates that slight undersizes can be allowed without reducing fatigue life.

A check of the nut measurements on the example specimens discussed above showed the nuts to be within the specified tolerance limits on all specimens except end BDOT. The minor diameter on the undersized failed end BDOT averaged 0.012 in. over the maximum tolerance. This combination of nut and bolt gave only 58 percent of the minimum amount of thread height engagement, taken as the minimum allowed major diameter less the maximum allowed minor diameter, with no adverse effects on fatigue life performance.

Although some very loose fitting nuts gave no reduction in fatigue life, one Type B specimen, B11, was fabricated with exceptionally ragged threads and had an average major diameter of only 1.685 in. which is 0.040 in. below the minimum allowed major diameter. This specimen failed by stripping in the nut under static loading at only 26 percent of the nominal yield strength of the bar. Therefore, static failure must be considered when establishing acceptability of any undersized anchor bolts.

The performance of the galvanized specimens was also reviewed considering the amount of overtapping measured on the galvanized nuts. Although both 1-3/8 in. and 2 in. galvanized nuts had been tapped oversized, no 1-3/8 in. nut measurements were found to exceed the maximum tolerance for uncoated threads and the 2 in. nuts only exceeded this tolerance by an average of 0.017 in. Since the corresponding galvanized bolts for each diameter were also at or over the nominal maximum diameter, the relative thread fit was greater than the minimum allowed in all cases. The minimum relative fit of the Type D and F specimens was 27% and 15%, respectively, greater than the minimum determined from the ANSI specification. The relative thread fit was calculated by subtracting the average minor nut diameter from the average major bolt diameter for each specimen end and comparing this value to a minimum engagement height taken as the ANSI minimum major bolt diameter less the maximum minor nut diameter for uncoated threads of each respective specimen type.

Although the thread fit for these galvanized bolts was acceptable, there is no ANSI limit on the amount of overtapping allowed on galvanized nuts to insure acceptable thread fits on anchor bolts. On the basis of manufacturer and designer consultation, Section 86 of the Standard Specifications for the State of California Department of Transportation (15) allows the pitch diameter of the galvanized nuts to be tapped over ANSI Standard: B1.1, Class 2B (internal threads) tolerances by the following maximum amounts:

5/8 inch through 1 inch . . 0.023-inch oversize
1-1/8 inch and larger . . . 0.033-inch oversize

If the galvanized nuts for specimen Types D and F had minor diameters tapped oversize by the maximum 0.033 in. tolerance recommended, the height of thread engagement obtained by using these nuts with the smallest allowed bolts would be 72 and 80 percent of the minimum engagement height as defined above for Types D and F, respectively. Although this oversizing can result in less than minimum ANSI uncoated thread engagement, it should be recalled that Specimen BDOT had only 58 percent of the specified minimum thread engagement and still performed satisfactorily under both static and fatigue loading. Therefore, these overtapping allowances seem to give adequate clearance for coated bolt threads and should not adversely affect fatigue behavior when used on bolts with major diameters greater than the ANSI minimum allowables for uncoated threads.

4.2 Effect of Differences in Thread Pitch

As discussed previously in Section 3.1, ultrasonic inspection of Type D specimens (1-3/8 in., A36, 6UNC cut threads) indicated that the first fatigue cracking for this type initiated near the free face of the nut and spread into multiple cracks before failure. In all other specimens monitored ultrasonically, the first crack initiated from the first engaged thread at the loaded face of the nut and cracking was limited to the first and second fully engaged threads. This difference in crack behavior indicates a load distribution within the Type D nuts which deviates from the distribution within the other specimen types.

The apparent net effect of this different load distribution was to cause multiple cracking to occur within the nut and to extend the bolt fatigue life. The fatigue life was extended since failure did not occur from the first crack formed. Although the fatigue life was extended over that of a specimen with a single crack, the rate of initiation and crack propagation of the second crack was probably increased by the load eccentricity within the nut due to the interior cracking.

Since the cracking of the Type D specimens began so far within the nut from the loaded face, it is reasonable to assume that the maximum thread load within the nut was also away from the loaded face. Sopwith[14] presents an analytical model for the distribution of loads in screw threads which gives the maximum thread loading and distrubution of thread loads within the nut. The load distribution depends on the proportions of the thread, the form of the thread, and the degree of lubrication.

This model can also be used to show analytically that the load distribution is highly dependent on the relative thread pitches of the nut and bolt. Thread pitch is defined as the peak to peak distance between threads or as the inverse of the number of threads per inch. Figure 44 shows schematically the thread shear load distribution within the nut length for threads with a standard uniform pitch, for a uniform difference in pitch, and for a uniform pitch with a slightly tapered minor nut diameter with the larger end at the bearing face. It is interesting to note that the slightly tapered nut with a uniform pitch gives a uniform thread shear force distribution and implies neglecting the influence of the axial force in the bar, that an equal probability of crack initiation exists along the full length of the nut, even at the free face.

Generally this figure shows that a large reduction in the maximum thread load can be made by using nuts with slightly larger pitch, nuts with a varying pitch, or tapered nuts with uniform pitch. Also, Sopwith indicated that these peak load reductions could be obtained with a uniform pitch difference or nut taper of only 1 in 1000.

Although none of these variations in pitch could be detected within the Type D threads where the nut could be removed from the failed end, the fabrication procedure following the galvanizing could possibly result in some pitch variations. One variation could result from using a tapered thread tap to oversize the galvanized nut. If the nut is tapped from the bearing face and not completely threaded through the nut, the oversizing process may leave the nut threads with the required variation in taper.

Also, if the nut threads were formed on a machine with a slightly different tool lead than the machine which fabricated the bolt threads, a uniform difference in pitch and reduction in peak thread load may result. These examples illustrate that differences in thread pitch may be responsible for the exceptional crack initiation behavior for the Type D specimen due to variations in peak thread shear load within the nut.

4.3 Effects of Residual Stresses

Specimens with rolled threads (Type E) endured over 11 and 16 million cycles at stress ranges of 15 and 10 ksi, respectively, with no failures. In addition, no crack indications were found in any of these specimens when inspected ultrasonically. It has been proposed previously[7] that specimens with rolled threads may partially attribute their long life and runout behavior at low stress ranges to the presence of compressive residual stresses that have been induced at the root of the thread profile by the thread rolling process. Although no qualitative values can be assigned to these stresses, they may be great enough to reduce the effective stress range at the thread root to a value below which fatigue cracks can not be initiated or to a point below which an existing crack will not propagate. In addition, rolled threads may also gain additional life over comparable cut threads due to the smoother root radius and its effect on fatigue crack initiation. Either of the above qualities resulting from rolled thread fabrication may be responsible for the higher fatigue limit or run out stress exhibited by the Type E specimens.

Although the statistical comparisons of the A36, 1-3/8 in. specimens with rolled and cut threads showed no significant difference in their fatigue behavior, the Type D specimens with cut threads were the type which exhibited multiple cracking before failure. Since the multiple cracking should tend to extend the fatigue life beyond that of a bolt with a single crack surface, comparisons of life made on a typical single crack basis would show rolled threads giving longer lives with run out at low stress ranges. However, the trade off of added fabrication cost with the increase in fatigue life should be considered before specifying rolled threads on anchor bolts. It may be more economical to increase the number or size of standard cut thread bolts rather than reducing the number of bolts by specifying rolled threads.

CHAPTER 5

COMPARISONS WITH PREVIOUS RESULTS

The results of the fatigue tests complied in this study were compared to the results obtained in previous investigations[13,16] and were seen to give very good correlations as shown in the plot of all test results in Fig. 45.

The low-cycle fatigue tests of large-diameter bolts[13] were done using high strength 4340 steels with varying yield strengths which ranged from 90 to 153 ksi. These specimens ranged in diameter from 1 to 5 in. and included threads which were machined, rolled, ground, and polished. Also, some specimens were tested using a taper in the nut threads.

Although the majority of these specimens were tested at stress ranges of 40 to 80 ksi with some tests at 18 to 30 ksi ranges, the results of these tests are seen to correlate well with the results of all high strength specimens tested in this study. Some of the specimens gave almost identical fatigue lives in both sets of data.

The fatigue data compiled by the United States Steel Corporation[16] was based on the behavior of A36, 1-1/2 in.-UNC-1A, threaded rods which were subjected to variable and/or constant amplitude loads. Since some of the specimens were subjected to variable loading, an effective stress range was calculated and reported for each specimen. The effective stress range, sometimes referred to as the root-mean-square stress range, is a constant stress range which would produce the same fatigue life as the random stress. Although all stresses were based on the tensile stress area, these rods were subjected to secondary bending stresses which were not included in the stresses plotted.

This data, as shown in Fig. 45, is seen to be slightly below the A36 test data generated in the current study. This difference is most likely due to the bending stresses which if included would increase the stress range.

It should also be noted from Fig. 45 that no apparent fatigue limit is evident even at very low effective stress ranges, 4 to 5 ksi. Also, all the threaded rods were reported to have failed at the first engaged thread at the bearing face of the nut as did the majority of anchor bolts in this study.

Considering the wide range in steels, diameters, threads, and testing techniques represented by these results in Fig. 45, their good correlation with the results of the present study provide additional confidence in the individual test results reported herein.

The allowable fatigue stress range for a Category E detail in the AASHTO fatigue specifications is shown by the dashed line in Fig. 45. This line corresponding to this category is seen to provide a reasonable lower bound for the anchor bolt data and is recommended for design.

CHAPTER 6

SUMMARY AND CONCLUSIONS

This study has covered many aspects of anchor bolt fatigue behavior by investigating a wide range of commonly used steels, diameters, thread types and loading. Statistical analysis was used to determine the significance of several design parameters, and supporting tests for mechanical properties, chemical composition and material toughness characteristics were also performed and reported. In addition, full-sized tension tests were used to verify static load capacity and ultrasonic inspection was used to detect crack initiation and growth within the fatigue specimens during the application of load cycles. The findings and conclusions of this study are listed as follows:

(1) Stress range was the most significant variable accounting for the greatest variation in fatigue life.

(2) The variation of bolt diameter had no significant effect on fatigue life.

(3) There was no significant difference in fatigue life between the two types of high strength steels tested.

(4) A significant difference in fatigue behavior was observed between high and low strength steel with the low strength steel giving significantly longer lives.

(5) Although confounded by additional variables to be resolved by future tests, thread series and thread forming method showed no significant difference in fatigue behavior.

(6) Investigations of thread measurements showed 63 percent of all specimens failed on the end with the smaller average major diameter. However, absolute values of thread major

diameter could not be used to predict the specimen fatigue life.

(7) Slight undersizes in bolt threads produced no adverse effects on fatigue life. Also, a specified oversizing of coated nuts by a maximum of 0.033 in. on the minor diameter should produce no adverse effects on fatigue life when used on coated bolts that fall within allowable ANSI minimum uncoated thread tolerances.

(8) Considerable scatter was observed in specimen fatigue behavior even from one end of a specimen to the other. In addition, the majority of specimens failed from a single crack which initiated and propagated from the first engaged thread at the bearing face of the nut. Cracks in the Type D specimens initiated at two-thirds the nut length from the loaded face and propagated into a series of multiple cracks before failure.

(9) All specimens failed by net section yielding.

(10) The log-log model relating stress range to cycle life was observed to give the best fit to the test data.

(11) Tension tests performed on full-size specimens gave results that correlated well with calculated loads which were based on tensile stress area.

(12) Charpy Impact tests indicated adequate toughness of all A193 Gr. B7 and A36 steels used in this study at all highway service temperatures. However, the heat treated 4340 steel was found to approach minimum toughness requirements within possible service temperature ranges. Therefore, Charpy V-notch tests of heat treated 4340 steels should be specified to insure sufficient toughness levels for the design service application.

(13) Ultrasonic inspection was found to be a very effective method for finding very small fatigue cracks. However, experience showed that inspections must be carefully and thoroughly performed by trained personnel in order to be fully effective and reliable.

(14) Ultrasonic inspections indicated the presence of fatigue cracks in 58 percent of all unfailed specimen ends.

(15) The results of the ultrasonic inspections were used to develop a method of determining inspection scanning levels, setting inspection intervals when no crack indications are found found, and estimating remaining fatigue life when a crack indication is detected during inspection.

(16) The Category E fatigue stress ranges in the present AASHTO fatigue specifications provide a lower bound to the anchor bolt fatigue data.

APPENDIX 1

TABLES

TABLE 1. SPECIMEN SERIES AND TEST VARIABLES

Specimen Series	Steel Type	Bolt Diameter	Thread Series	Forming Method
A	A193 Gr. B7	1-3/8 in.	8UN	Cut
B	A193 Gr. B7	1-3/4 in.	8UN	Cut
C	4340	1-3/8 in.	8UN	Cut
D	A36*	1-3/8 in.	6UNC	Cut
E	A36*	1-3/8 in.	8UN	Rolled
F	A36*	2 in.	4-1/2UNC	Cut

*Hot Dipped Galvanized

TABLE 2. INITIAL EXPERIMENT DESIGN

Stress Range (ksi)	Specimen Series					
	A	B	C	D	E	F
30	2*	2	2	2	2	2
20	2	2	2	2	2	2
10	2	2	2	2	2	2

*Number of Replicates

TABLE 3. FINAL EXPERIMENT DESIGN

Stress Range (ksi)	Specimen Series					
	A	B	C	D	E	F
30	2	2	2			
25				1 (2)*	(3)	1
20	2	2	2	3	3 (1)	3
15					1	
10	2	2	2	2	2	2

*Numbers in parenthesis indicate data from retested specimens.

TABLE 4. MECHANICAL PROPERTIES OF TEST MATERIALS

Specimen Series	Steel Type	Nominal Yield (ksi)	Reporting Test	Dynamic Yield (ksi)	Static Yield (ksi)	0.2% Off-set Yield (ksi)	Ultimate Stress (ksi)	Rupture Stress (ksi)	Percent Elong.* (%)	Reduction of Area (%)
A	A193 Gr. B7	105	Mill	--	--	127.5	140.0	--	22.0	58.6
			Lab.	--	--	114.5	139.9	216.4	20.9	55.3
B	A193 Gr. B7	105	Mill	--	--	117.0	136.2	--	19.2	64.0
			Lab.	--	--	109.5	132.2	235.9	24.4	63.9
C	Heat-treated 4340	150	Mill**	--	--	--	--	--	--	--
			Lab.	--	--	171.3	181.4	253.0	15.0	49.6
D	A36	36	Mill	45.79	--	--	69.85	--	21.0†	--
			Lab.	38.3	34.5	--	60.1	96.5	41.9	51.8
F	A36	36	Mill	41.72	--	--	65.97	--	31.0†	--
			Lab.	26.7	23.2	--	43.5	100.2	50.0	73.8

*2 in. gage length except where noted.
**Certified Heat Treatment: Hardening at 1550 ^{o}F for 2 hrs and quenched in oil; first tempering at 900 ^{o}F for 3 hrs and quenched in air for final Brinell hardness of 363-388.
†8 in. gage length.

TABLE 5. CHEMICAL COMPOSITION ANALYSIS FOR ALL TEST SERIES

Specimen Series	Analysis Used	C	Mn	P	S	Si	Ni	Cr	Mo	Cu	V	B	Pb
A 1-3/8 A193 Gr. B7	Mill Report	0.41	0.92	0.012	0.024	0.30	--	1.06	0.17	--	--	--	
	Lab Analysis	0.41	0.98	0.012	0.026	0.28	0.14	1.01	0.17	0.19	≤0.01	0.0005	
	ASTM A193-73 Check Var.	0.38-0.48 ±0.02	0.75-1.00 ±0.04	0.04 max +0.005	0.04 +0.005	0.20-0.35 ±0.02	-- --	0.80-1.10 ±0.05	0.15-0.25 ±0.02	--	--	--	
B 1-3/4 A193 Gr. B7	Mill Report	0.41	0.90	0.010	0.028	0.28	0.16	0.97	0.22	--	--	--	
	Lab Analysis	0.45	0.95	0.012	0.033	0.28	0.14	0.92	0.20	0.15	<0.01	0.0005	
	ASTM A193-73 Check Var.	0.38-0.48 ±0.02	0.75-1.00 ±0.04	0.035 max +0.005	0.04 +0.005	0.20-0.35 ±0.02	--	0.80-1.10 ±0.05	0.15-0.25 ±0.02	--	--	--	
C 1-3/8 4340	Mill Report	0.40	0.69	0.015	0.015	0.27	1.76	0.78	0.25	--	--	--	
	Lab Analysis	0.41	0.95	0.013	0.030	0.32	1.70	0.87	0.18	0.09	<0.01	0.0005	*
	AISI 4340	0.38-0.43	0.60-0.80	0.04 max	0.04 max	0.20-0.35	1.65-2.00	0.70-0.90	0.20-0.30	--	--	--	
D 1-3/8 A36	Mill Report	0.22	0.79	0.007	0.028	--	--	--	--	--	--	--	
	Lab Analysis	0.22	0.85	0.014	0.040	0.05	0.13	0.09	0.01	0.28	<0.01	0.0008	
	ASTM A36-74 Check Var.	0.27 max ±0.02	0.60-0.90 ±0.03	0.04 max +0.008	0.05 max +0.008	--	--	--	--	--	--	--	
F 2 A36	Mill Report	0.18	0.80	0.007	0.028	--	--	--	--	--	--	--	
	Lab Analysis	0.06	0.38	0.005	0.018	<0.01	0.01	0.02	<0.01	0.01	<0.01	<0.0005	
	ASTM A36-74 Check Var.	0.28 max ±0.02	0.60-0.90 ±0.03	0.04 max +0.008	0.05 max +0.008	--	--	--	--	--	--	--	

*Lead detected in analysis; no percentage reported.

TABLE 6. SPECIMEN DESIGNATION

Example: A31A

A	3	1	R	A
Test Series	Stress Range	Specimen Number	Retest Indication (Optional)	Specimen End

Test Series:	A - A193, 1-3/8"	8UN - Cut Threads
	B - A193, 1-3/4"	8UN - Cut Threads
	C - 4340, 1-3/8"	8UN - Cut Threads
	D - A36, 1-3/8"	6UNC - Cut Threads
	E - A36, 1-3/8"	8UNC - Rolled Threads
	F - A36, 2"	4-1/2UNC - Cut Threads
S_r	1, 2, 3 . . . indicate first, second . . . stress range	
Replicate No.	1 or 2	
Specimen End	A or B	
Retest Mark (Optional)	R	

Example: C32A

4340 steel, 1-3/8" diameter with 8UN cut threads

Third magnitude of stress range (30 ksi)

Specimen No. 2

End A

Specimen is not retested (R is deleted)

TABLE 7. INDEX TO TEST SPECIMENS BY IDENTIFYING CODE

Specimen Series	Stress Range (ksi)				
	30	25	20	15	10
A	A31		A21		A11
	A32		A22		A12
B	B31		B21		B11
	B32		B22		B12*
C	C31		C21		C11
	C32		C22		C12
		D32	D31		
D		D22R	D21		D11
		D11R	D22		D12
E		E32R	E31	E32	E11
		E11R	E21		E12
		E12R	E22		
			E31R		
			F31		F11
F		F32	F21		F12
			F22		

*Extra fatigue specimen, designated BDOT-BBAR, also tested.

TABLE 8. SUMMARY OF ANCHOR BOLT FAILURE DATA

Failed End Designation	Stress Range (ksi)	Max. Stress (ksi)	Min. Stress (ksi)	Failure Cycles (N_f)	Crack Detected (N_c)	Defect Rating (db)
A32A	30.0	78.8	48.8	59,760	27,500	28
A32B	30.0	78.8	48.8	65,270	23,330	30
A21B	20.0	78.8	58.8	189,270	68,720	27
A22A	20.0	78.8	58.8	176,810		
A11	10.0	78.8	68.8	11,800,000*		
A12A	10.0	78.8	68.8	2,012,500	1,357,500	15
B31B	30.0	78.8	48.8	63,610		
B32A	30.0	78.8	48.8	61,180	30,000	35
B21A	20.0	78.8	58.8	138,810		
B22B	20.0	78.8	58.8	181,500	100,000	34
B11A	10.0	78.8	68.8	1,402,700		
B12	10.0	78.8	68.8	Threads stripped during static loading		
B**	10.0	78.8	68.8	2,031,000		
C31	30.0	112.5	82.5	54,000		
C32	30.0	112.5	82.5	38,720		
C21	20.0	112.5	92.5	114,440		
C22	20.0	112.5	92.5	121,120		
C11	10.0	112.5	102.5	1,203,100		
C12	10.0	112.5	102.5	2,774,540		
D32A	25.0	27.0	2.0	793,290		
D22B-R	25.0	27.0	2.0	224,660	55,000	40
D11B-R	25.0	27.0	2.0	240,060	178,400	33
D31A	20.0	27.0	7.0	1,794,410	850,000	25
D21A	20.0	27.0	7.0	1,137,500	680,000	11
D22B	20.0	27.0	7.0	1,753,460	735,400	21
D11B	10.0	27.0	17.0	15,838,480	7,000,000	19
D12A	10.0	27.0	17.0	11,205,890	9,762,940	15
E32A-R	25.0	27.0	2.0	720,580		
E11A-R	25.0	27.0	2.0	347,690		
E12A-R	25.0	27.0	2.0	296,440	206,000	34
E31A	20.0	27.0	7.0	579,140		
E31A-R	20.0	27.0	7.0	366,590		
E21B	20.0	27.0	7.0	4,907,050	1,574,500	26
E22A	20.0	27.0	7.0	509,330		
E32	15.0	27.0	12.0	11,035,420*		
E11	10.0	27.0	17.0	16,392,620*		
E12	10.0	27.0	17.0	17,202,204*		
F32A	24.0	27.0	3.0	131,560	40,000	38
F31A	20.0	27.0	7.0	240,360	130,700	33
F21A	20.0	27.0	7.0	227,340		
F22A	20.0	27.0	7.0	1,028,540		
F11B	10.0	27.0	17.0	3,163,240		
F12A	10.0	27.0	17.0	1,625,300	704,500	28

-- Data not available

* Specimen removed before failure; no cracks detected

** Designates extra fatigue test specimen, noted as BDOT-BBAR.

TABLE 9. SUMMARY OF SPECIMENS WITH CRACKS AT THE UNFAILED END

	Specimen Series					
	A	B	C	D	E	F
Number of Specimens	6	6	6	6	6	6
Percent of Specimens Cracked on Unfailed End	66	66	50	83	0	83

Percentage of all specimens cracked on unfailed end = 58%.

TABLE 10. ANALYSIS OF VARIANCE STRESS RANGE VS. THREAD FORMING METHOD

Factorial I

A36, 1-3/8 in.: Cut Threads and Rolled Threads Confounded by Thread Series

Source of Variation	Sum of Squares	Degree of Freedom	Mean Squares	F Calc.	F* Tab.
Stress Range	0.7215	1	0.7215	9.3846	5.32
Forming Method	0.0149	1	0.0149	0.1943	5.32
Interaction	0.0679	1	0.0679	0.8827	5.32
Residual	0.6151	8	0.0769		
Total	1.4194	11	0.1290		

*α = 0.05

TABLE 11. ANALYSIS OF VARIANCE STRESS RANGE VS. BAR DIAMETER

Factorial II

A193 Gr. B7, 8UN, Cut Threads: 1-3/8 in. and 1-3/4 in.

Source of Variation	Sum of Squares	Degree of Freedom	Mean Squares	F Calc.	F^* Tab.
Stress Range	5.9414	2	2.9707	56.3395	5.14
Bar Diameter	0.0910	1	0.0910	1.7252	5.99
Interaction	0.1247	2	0.0623	1.1822	5.14
Residual	0.3164	6	0.0527		
Total	6.4734	11	0.5885		

Factorial III

A36, Galv., Cut Threads: 1-3/8 in. and 2 in.

Confounded by Thread Series

Source of Variation	Sum of Squares	Degree of Freedom	Mean Squares	F Calc.	F^* Tab.
Stress Range	1.4208	1	1.4208	39.7152	7.71
Bar Diameter	0.9586	1	0.9586	26.7965	7.71
Interaction	0.0118	1	0.0118	0.3290	7.71
Residual	0.1431	4	0.0358		
Total	2.5343	7	0.3620		

$^*\alpha = 0.05$

TABLE 12. ANALYSIS OF VARIANCE STRESS RANGE VS. TYPE OF STEEL

Factorial IV

1-3/8 in., 8UN, Cut Threads: A193 Gr. B7 and 4340

Source of Variation	Sum of Squares	Degree of Freedom	Mean Squares	F Calc.	F^* Tab.
Stress Range	6.6065	2	3.3033	53.1199	5.14
Type of Steel	0.1888	1	0.1888	3.0365	5.99
Interaction	0.0475	2	0.0237	0.3818	5.14
Residual	0.3731	6	0.0622		
Total	7.2159	11	0.6560		

Factorial V

1-3/8 in., Cut Threads: A193 Gr. B7, 4340 and A36

Confounded by Thread Series

Source of Variation	Sum of Squares	Degree of Freedom	Mean Squares	F Calc.	F^* Tab.
Stress Range	4.1671	1	4.1671	66.4512	5.99
Type of Steel	2.0908	2	1.0454	16.6705	5.14
Interaction	0.1281	2	0.0641	1.0214	5.14
Residual	0.3763	6	0.0627		
Total	6.7623	11	0.6148		

$^*\alpha = 0.05$

TABLE 13. ANALYSIS OF VARIANCE STRESS RANGE VS. TYPE OF STEEL

Factorial VI

1-3/8 in., 8UN: A193 Gr. B7, 4340, and A36

Confounded by Forming Method

Source of Variation	Sum of Squares	Degree of Freedom	Mean Squares	F Calc.	F^* Tab.
Stress Range	4.7196	1	4.7196	47.4355	5.99
Type of Steel	2.0326	2	1.0163	10.2146	5.14
Interaction	0.0448	2	0.0224	0.2254	5.14
Residual	0.5970	6	0.0995		
Total	7.3941	11	0.6722		

Factorial VII

1-3/8 in., Cut Threads: A193 Gr. B7 and A36

Confounded by Thread Series

Source of Variation	Sum of Squares	Degree of Freedom	Mean Squares	F Calc.	F^* Tab.
Stress Range	2.7492	1	2.7492	35.4613	7.71
Type of Steel	0.9518	1	0.9518	12.2768	7.71
Interaction	0.1279	1	0.1279	1.6495	7.71
Residual	0.3101	4	0.0775		
Total	4.1390	7	0.5913		

$^*\alpha = 0.05$

TABLE 14. REGRESSION ANALYSIS RESULTS
OF INDIVIDUAL TEST SERIES

Model A: $\text{Log } N = B_1 + B_2 S_r$

Model B: $\text{Log } N = B_1 + B_2 \text{ Log } S_r$

Model	B_1	B_2	Correlation Coefficient	Standard Error of Est.
		Series A - 5 Specimens		
A	6.85208	-0.0712851	0.96807	0.17832
B	9.41167	-3.14801	0.99643	0.06003
		Series B - 6 Specimens		
A	6.83995	-0.0716135	0.096567	0.19264
B	9.24365	-3.04591	0.99096	0.09947
		Series C - 6 Specimens		
A	6.93252	-0.0800791	0.94961	0.26431
B	9.63964	-3.42128	0.97886	0.17247
		Series D - 8 Specimens		
A	8.20595	-0.104603	0.96038	0.20432
B	11.0020	-3.82111	0.94508	0.23963
		Series E - 7 Specimens		
A	7.16156	-0.0615184	0.39546	0.41832
B	10.0607	-3.17400	0.39546	0.41832
		Series F - 6 Specimens		
A	7.20542	-0.0831979	0.88501	0.28811
B	9.24874	-2.87129	0.87403	0.30067
		All Series - 38 Specimens		
A	7.26453	-0.0793083	0.79804	0.40734
B	9.64392	-3.11698	0.78312	0.42037

TABLE 15. REGRESSION ANALYSIS RESULTS FOR EFFECTS OF STEEL TYPES

Model A: $\text{Log } N = B_1 + B_2 S_r$

Model B: $\text{Log } N = B_1 + B_2 \text{ Log } S_r$

Model	B_1	B_2	Correlation Coefficient	Standard Error of Est.
		A193 Gr. B7 Steel - 11 Specimens		
A	6.84277	-0.0713277	0.96689	0.16493
B	9.29417	-3.07319	0.99268	0.07807
		4340 Steel - 6 Specimens		
A	6.93252	-0.0800791	0.94961	0.26431
B	9.63964	-3.42128	0.97886	0.17247
		All A36 Steel - 21 Specimens		
A	7.54132	-0.0815412	0.75528	0.38561
B	9.77733	-3.01418	0.75351	0.38681
		All High Strength Steel - 17 Specimens		
A	6.87288	-0.0742520	0.95558	0.19558
B	9.40879	-3.18884	0.98266	0.12307

TABLE 16. REGRESSION ANALYSIS RESULTS FOR EFFECTS OF BAR DIAMETER

Model A: $\text{Log } N = B_1 + B_2 S_r$

Model B: $\text{Log } N = B_1 + B_2 \text{ Log } S_r$

Model	B_1	B_2	Correlation Coefficient	Standard Error of Est.
	1-3/8 in. - 8UN - A193 Gr. B7 - 5 Specimens			
A	6.85208	-0.0712851	0.96807	0.17832
B	9.41167	-3.14801	0.99643	0.06003
	1-3/4 in. - 8UN - A193 Gr. B7 - 6 Specimens			
A	6.83995	-0.0716135	0.96567	0.19264
B	9.24365	-3.04591	0.99096	0.09947
	1-3/8 in. - 6UNC A36 - 8 Specimens			
A	8.20595	-0.104603	0.96038	0.20432
B	11.0020	-3.82111	0.94508	0.23963
	2 in. - 4-1/2UNC A36 - 6 Specimens			
A	7.20542	-0.0831979	0.88501	0.28811
B	9.24874	2.87129	0.87403	0.30067
	All 1-3/8 in. High Strength Steel - 11 Specimens			
A	6.89072	-0.0756229	0.95100	0.21541
B	9.50264	-3.26831	0.97938	0.14076
	All 1-3/8 in. - A36 Steel - 15 Specimens			
A	8.10884	-0.101945	0.86208	0.30798
B	11.0302	-3.86892	0.86060	0.30951
	All 1-3/8 in. - 8UN - 18 Specimens			
A	7.01111	-0.0706487	0.75790	0.41364
B	9.22598	-2.85265	0.73204	0.43196
	All 1-3/8 in. - 26 Specimens			
A	7.48188	-0.0853601	0.78565	0.44133
B	10.0637	-3.36891	0.76614	0.45846

TABLE 17 (Continued)

Failed End	Cycles to Failure	Reference Flaw, db	Crack Distance in.	Percent Cycle Life	Defect Rating, db
D11B*	15,838,480	6	2.5	44	21
				49	16
				54	15
				69	9
				87	3
				100	3
D12A*	11,205,890	6	4.0	87	16
				93	10
				99	10
				100	0
E21B	4,907,050	6	4.25	32	26
				45	27
				61	24
				77	23
				88	20
				100	6
E12A-R**	296,440	6	3.5	69	34
				76	33
				80	30
				86	28
				92	20
				99	0
				100	0
F31A	240,360	6	4.25	54	34
				58	30
				62	30
				67	27
				100	10
F32A	131,560	6	2.25	30	39
				42	32
				46	29
				51	29
				53	31
				57	28
				65	27
				73	25
				84	19
				91	8
				98	7
				100	7

TABLE 17 (Continued)

Failed End	Cycles to Failure	Reference Flaw, db	Crack Distance, in.	Percent Cycle Life	Defect Rating, db
F12A	1,625,300	6	4.5	43	28
				88	9
				100	--

*Indicates multiple crack data.

**Indicates elevated temperature and bending data.

A P P E N D I X 2

FIGURES

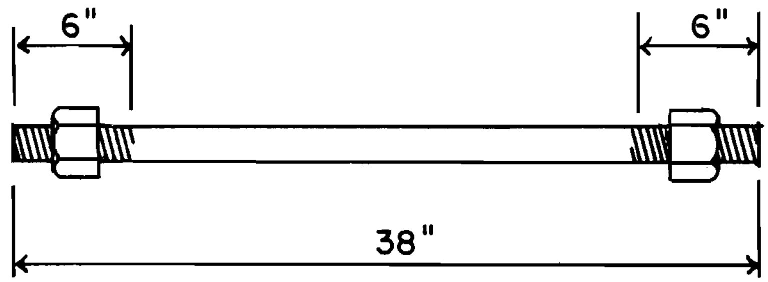

Fig. 1. Basic Test Specimen.

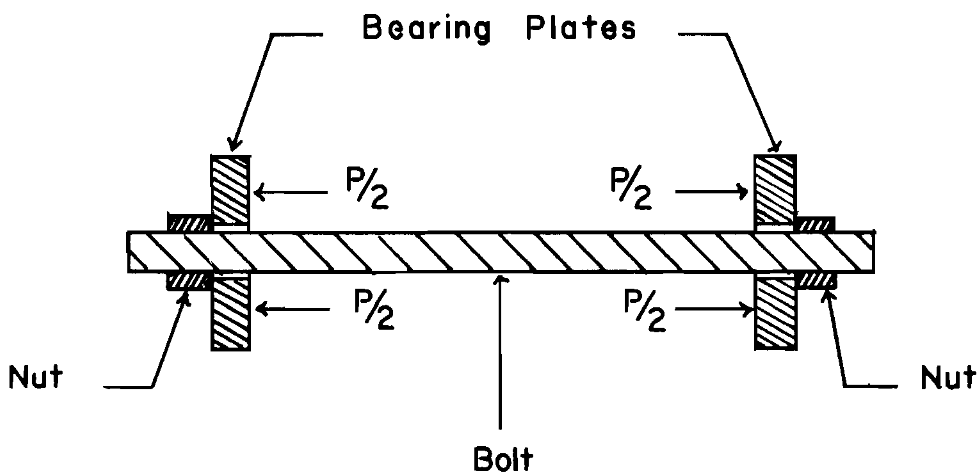

Fig. 2. Specimen Loading Geometry.

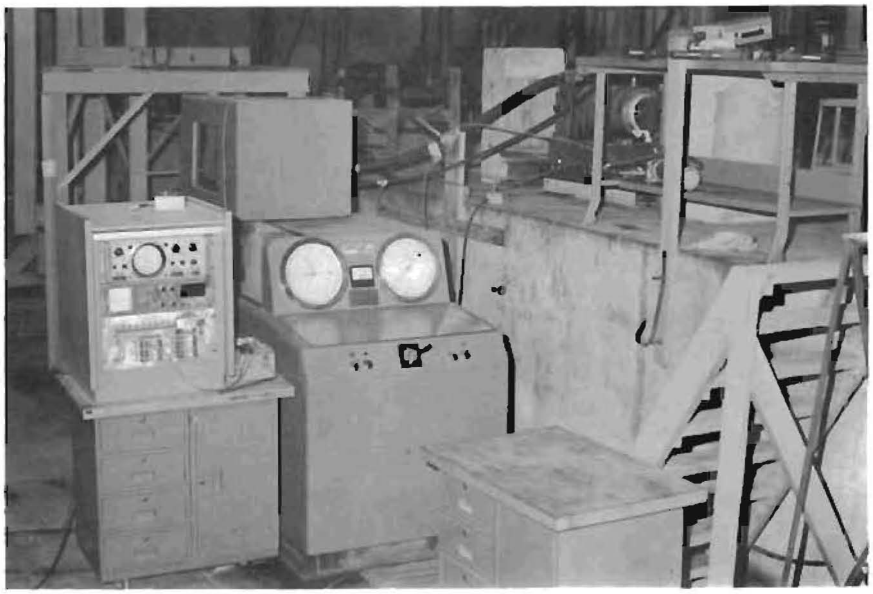

Fig. 3. Fatigue Loading System.

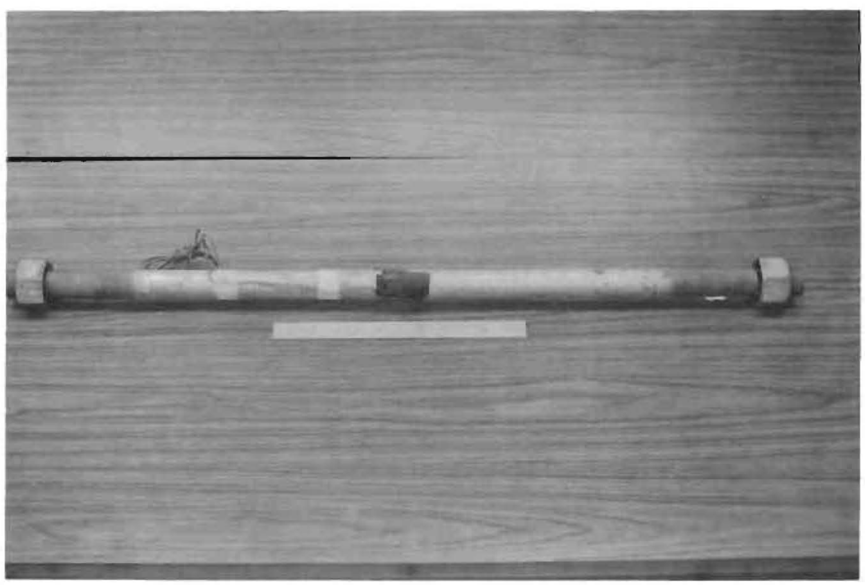

Fig. 4. Strain-gaged Specimen Ready for Testing.

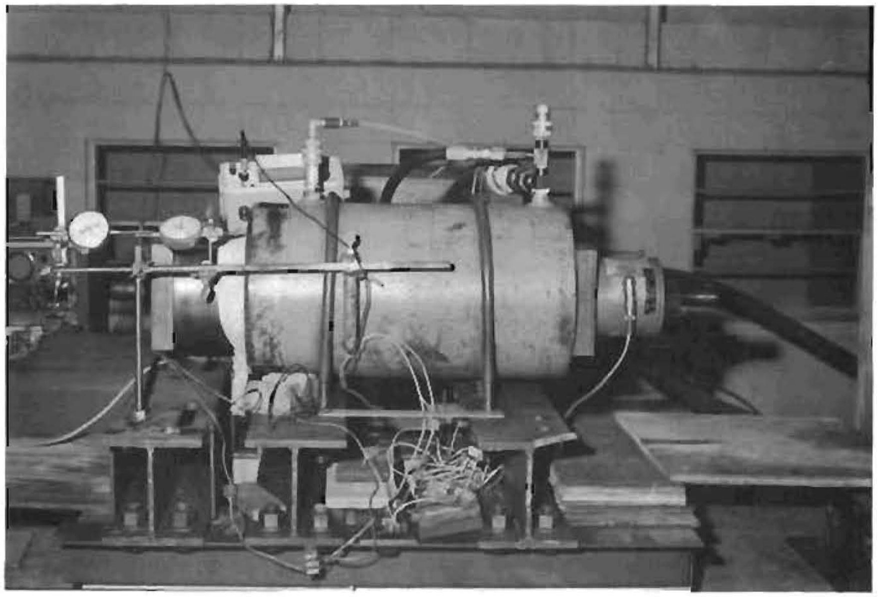

Fig. 5. Fatigue Test Loading Ram.

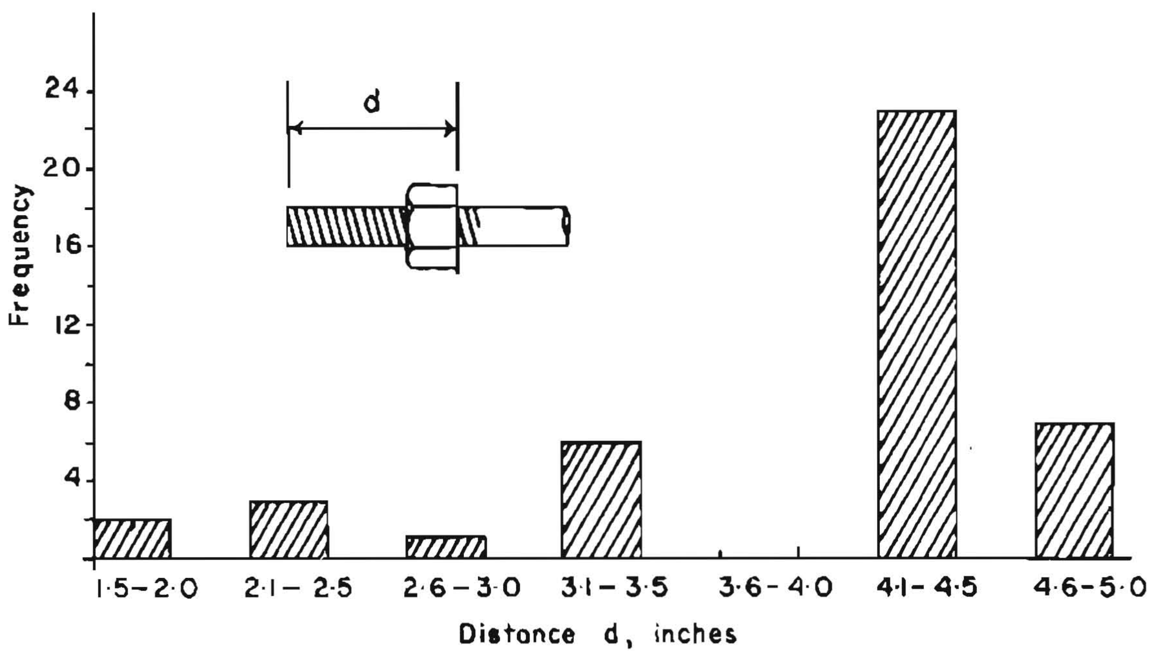

Fig. 6. Distribution of Nut Location on Fatigue Specimens.

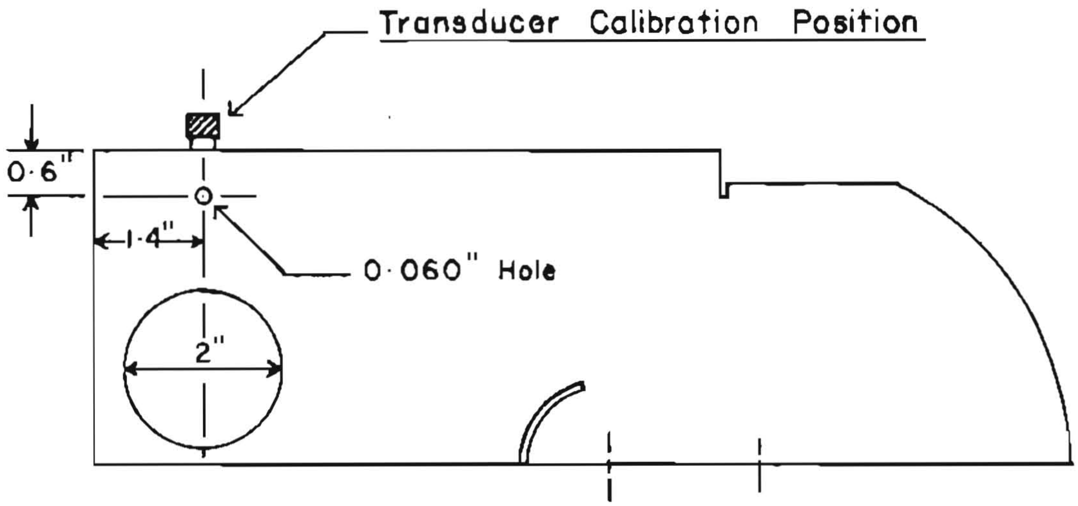

Fig. 7. Reference Flaw Calibration Position - IIW - Type I Ultrasonic Reference Block.

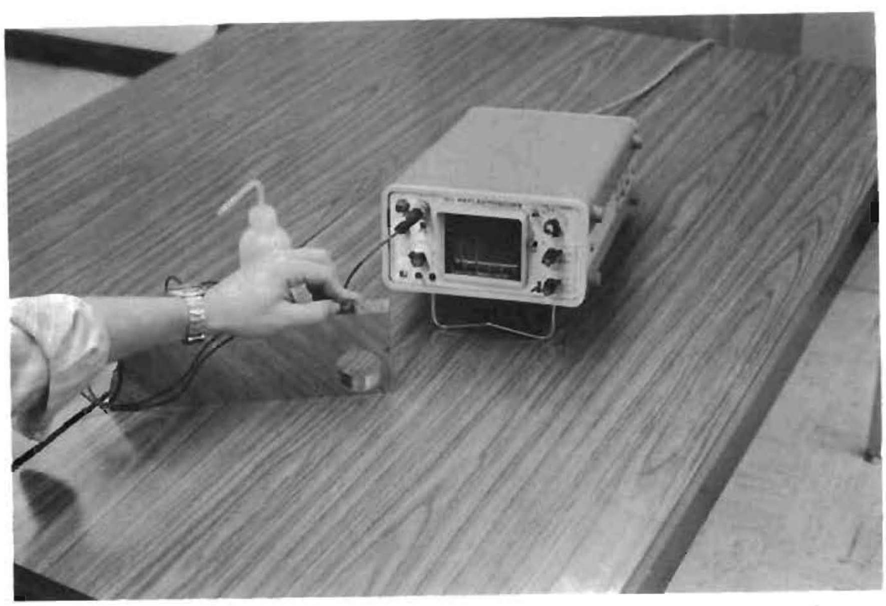

Fig. 8. Ultrasonic Inspection Unit Positioned for Calibration.

Fig. 9. Ultrasonic Inspection of Test Anchor Bolts.

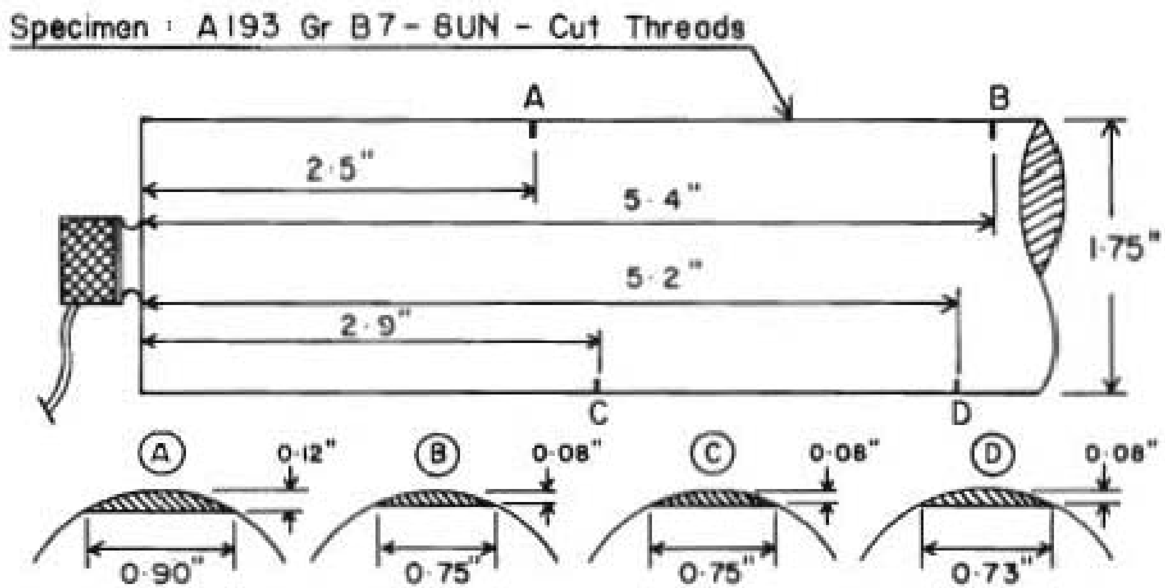

Defect Rating (Ref. Level = 6 db., Test Calibration)			
15 db.	32 db.	18 db.	28 db.

Fig. 10. Simulated Flaw Correlation for Ultrasonic Inspection.

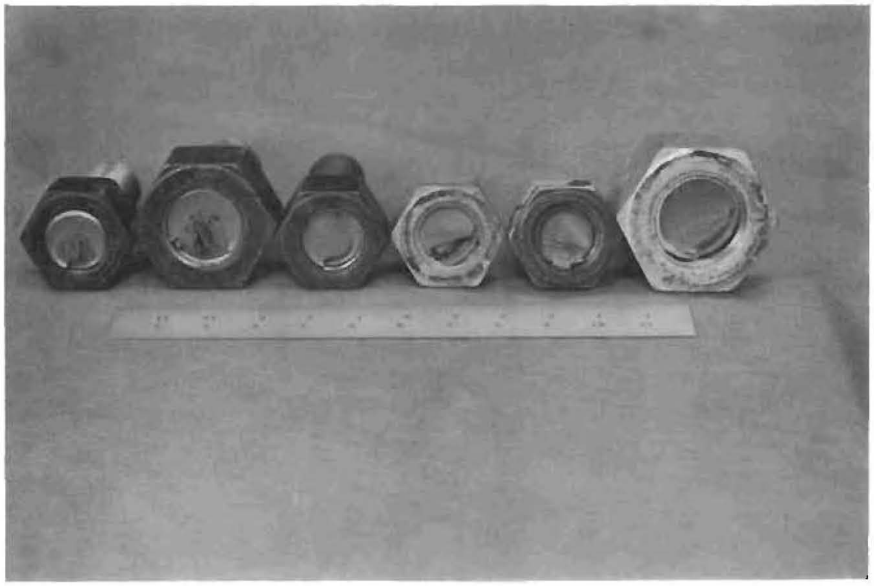

Fig. 11. Characteristic Failure Surface for Each Specimen Type. (Left to Right: Types A, B, C, D, E, and F)

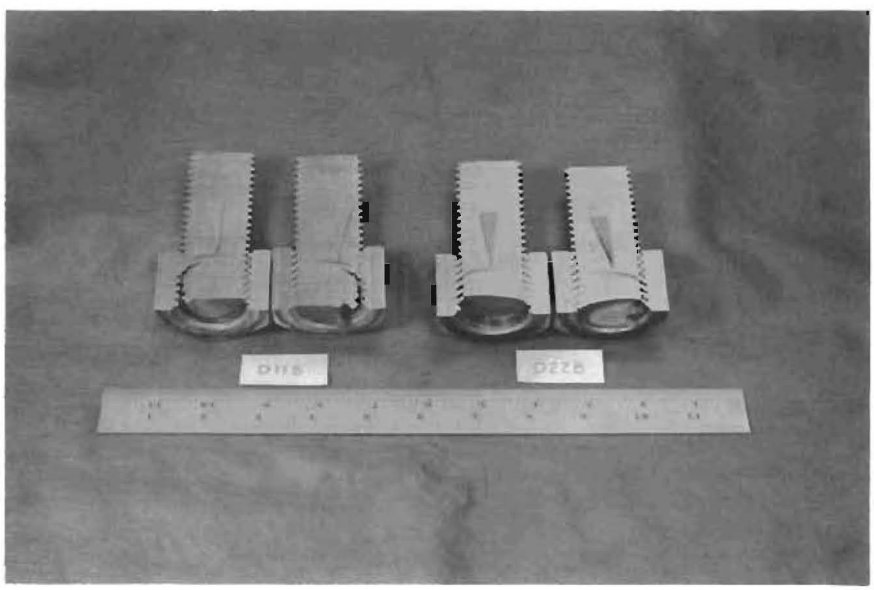

Fig. 12. Cross Sections of Type D Failed Ends.

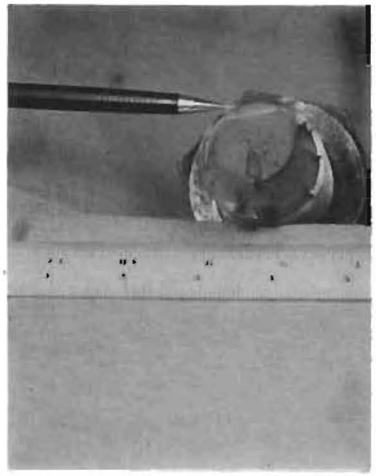

Crack Stage I
End: B32A

Crack Stage II
End: B32B

Fig. 13. Crack Growth Stages for Opposite Specimen Ends.

Factorial I

Common: Diameter - 1-3/8 in.
Steel - A36

Confounded by: Threads, 6UNC Vs. 8UN

Sr (ksi) \ Series	D	E
	Cut	Rolled
25	3*	3
20	3	4

*Number of Replicates

Fig. 14. Analysis of Variance for Effects of Forming Method.

Factorial II

Common: Steel - A193 Gr. B7
Threads - 8UN
Forming - Cut Threads

Sr (ksi) \ Series	A 1-3/8 in.	B 1-3/4 in.
30	2*	2
20	2	2
10	2	2

Factorial III

Common: Steel - A36
Forming - Cut
Galvanized

Confounded by: Threads - 6UNC Vs. 4-1/2UNC

Sr (ksi) \ Series	D 1-3/8 in.	F 2 in.
20	3*	2
10	2	2

*Number of replicates

Fig. 15. Analysis of Variance for Effects of Diameter.

Factorial IV

Common: Diameter - 1-3/8 in.
Forming - Cut
Threads - 8UN

Sr (ksi) \ Series	A	C
	A193 Gr. B7	4340
30	2*	2
20	2	2
10	2	2

Factorial V

Common: Diameter - 1-3/8 in.
Forming - Cut

Confounded by: Threads - 8UN vs. 6UNC

Sr (ksi) \ Series	A	C	D
	A193 Gr. B7	4340	A36
20	2*	2	3
10	2	2	2

*Number of replicates

Fig. 16. Analysis of Variance for Effects of Steel Types.

Factorial VI

Common: Diameter - 1-3/8 in.
Threads - 8UN

Confounded by: Forming - Cut vs. Rolled

Sr (ksi) / Series	A	C	E
	A193 Gr B7	4340	A36
20	2*	2	4
10	2	2	2

Factorial VII

Common: Diameter - 1-3/8 in.
Forming - Cut

Confounded by: Threads - 8UN vs. 6UNC

Sr (ksi) / Series	A	D
	A193 Gr. B7	A36
20	2*	3
10	2	2

*Number of replicates

Fig. 17. Analysis of Variance for Effects of Steel Types.

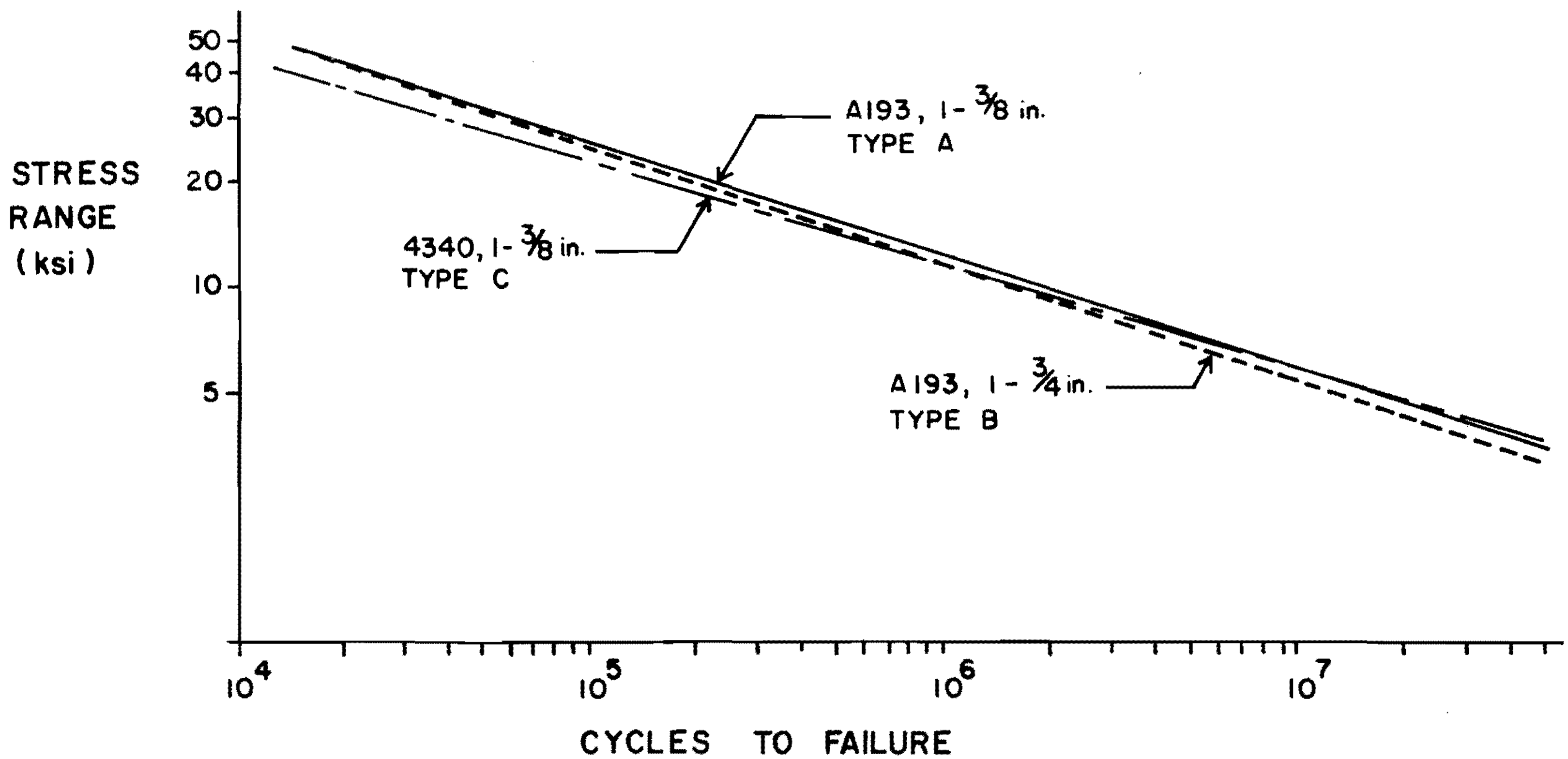

Fig. 18 Mean Regression Lines: A193 Gr. B7 and Heat-treated 4340 Steels.

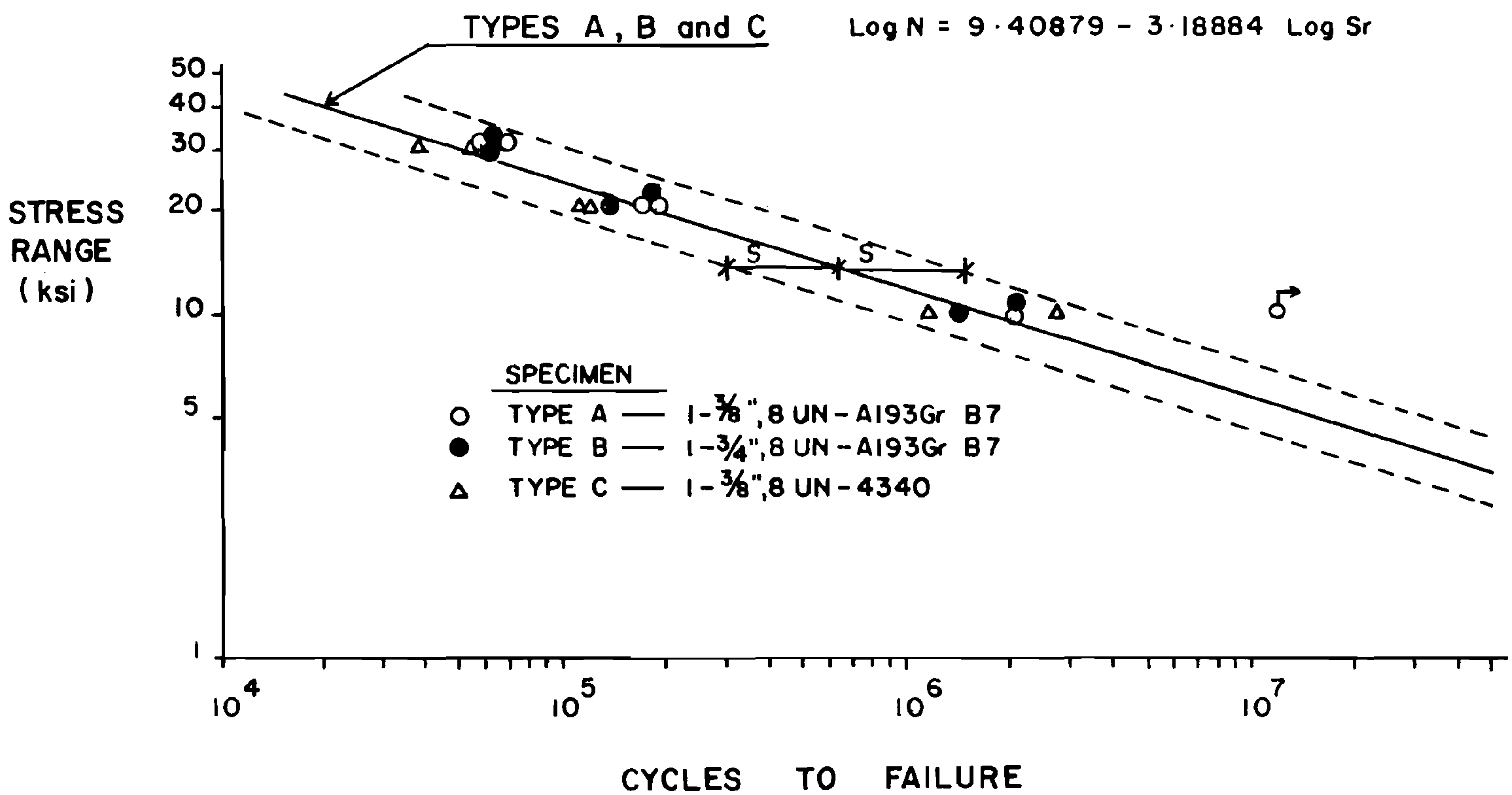

Fig. 19. Fatigue Test Results and Mean Regression Line for All High Strength Steel.

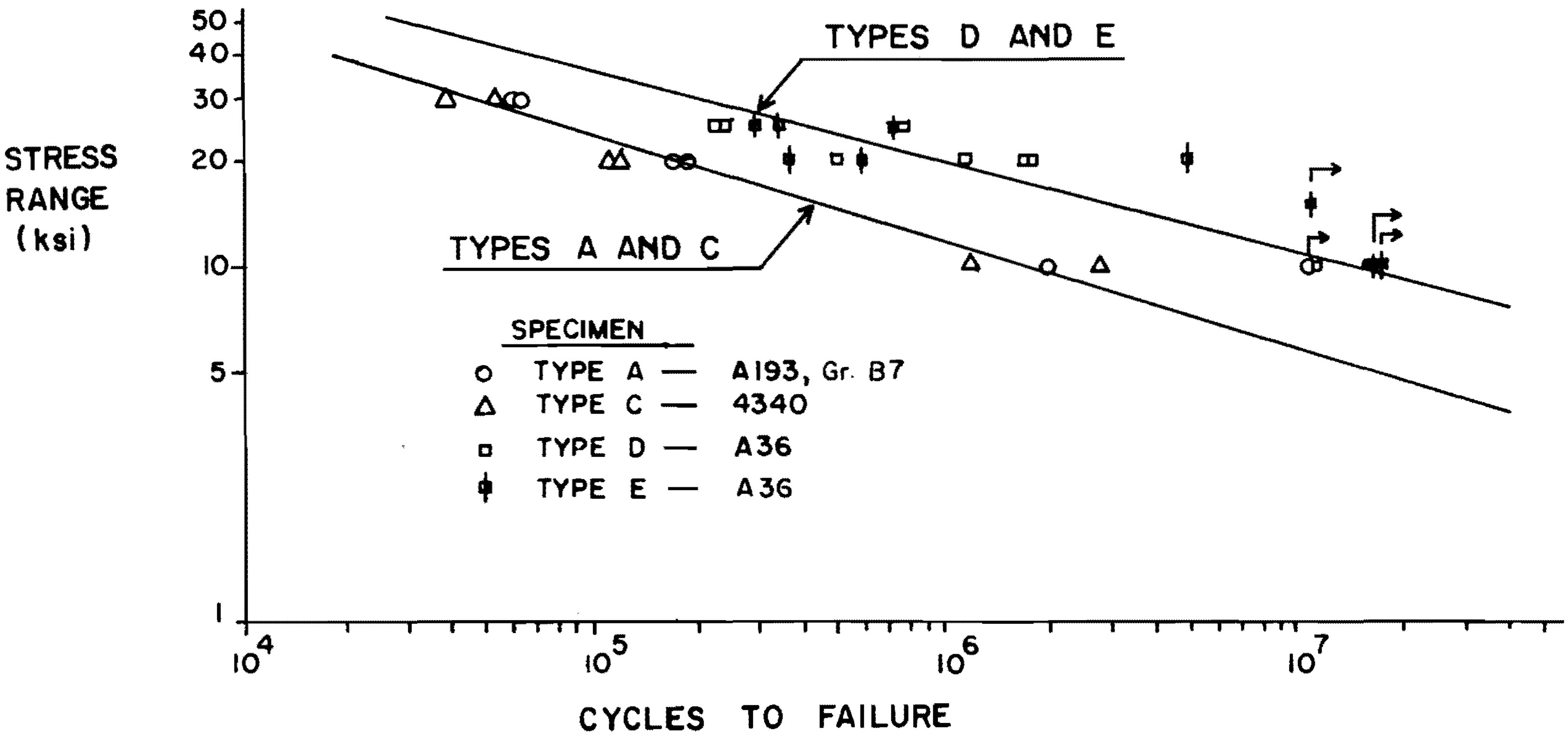

Fig. 20. Fatigue Test Results for All High Strength and Low Strength Steels at 1-3/8 in. Diameter.

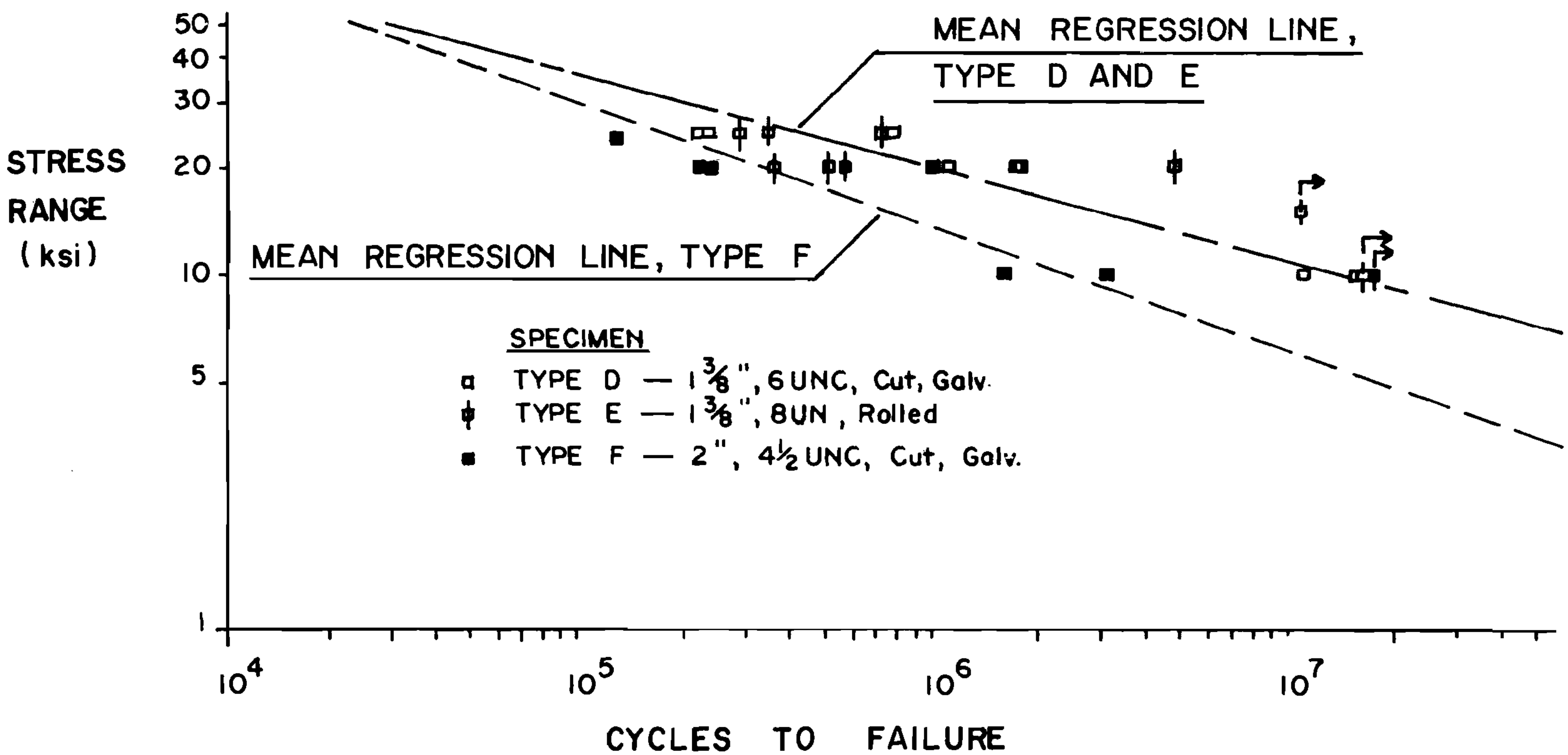

Fig. 21. Fatigue Results of All A36 Steel by Diameter.

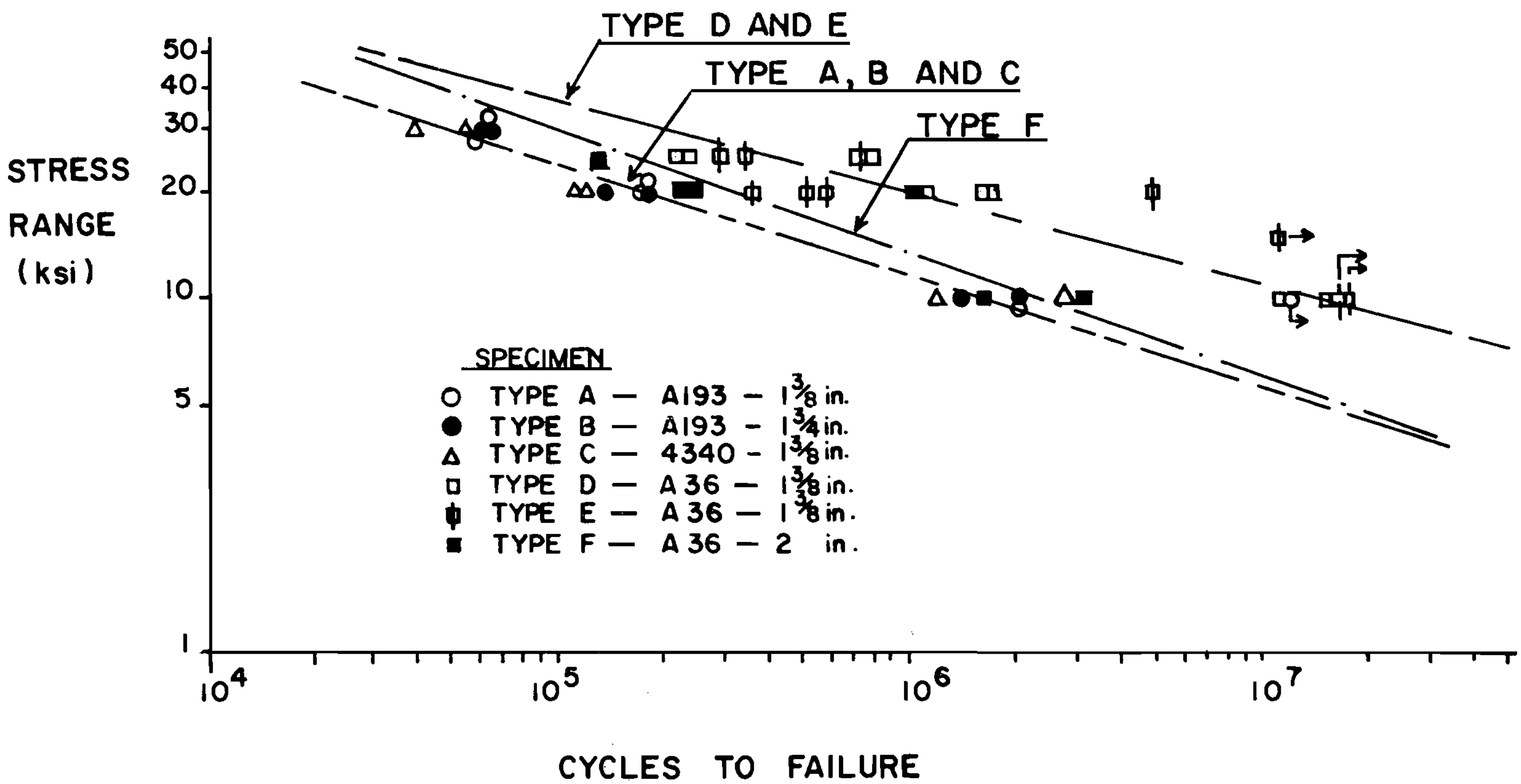

Fig. 22. Fatigue Test Results: High Strength and A36 Steel.

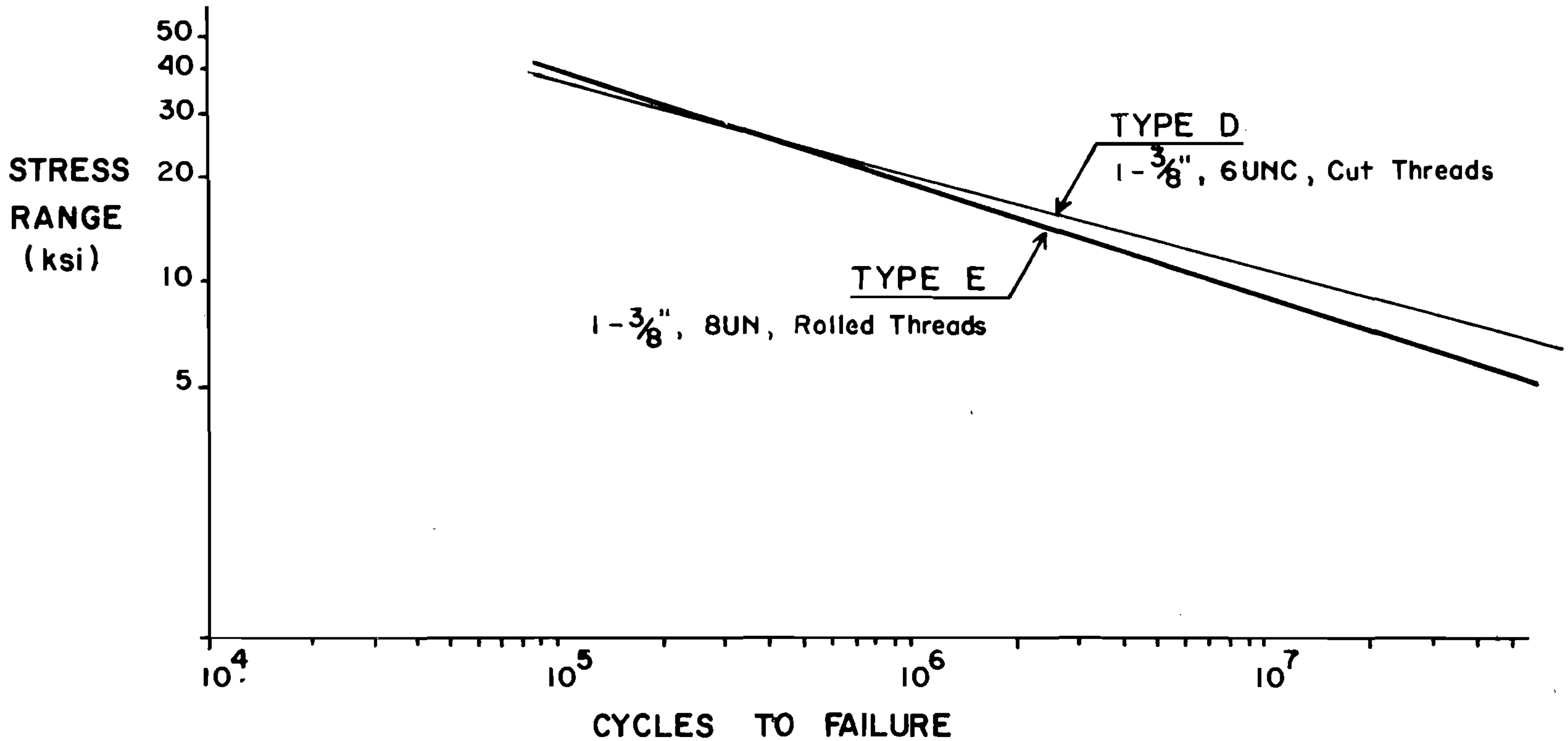

Fig. 23. Mean Regression Lines: A36, 1-3/8 in., Rolled and Cut Threads.

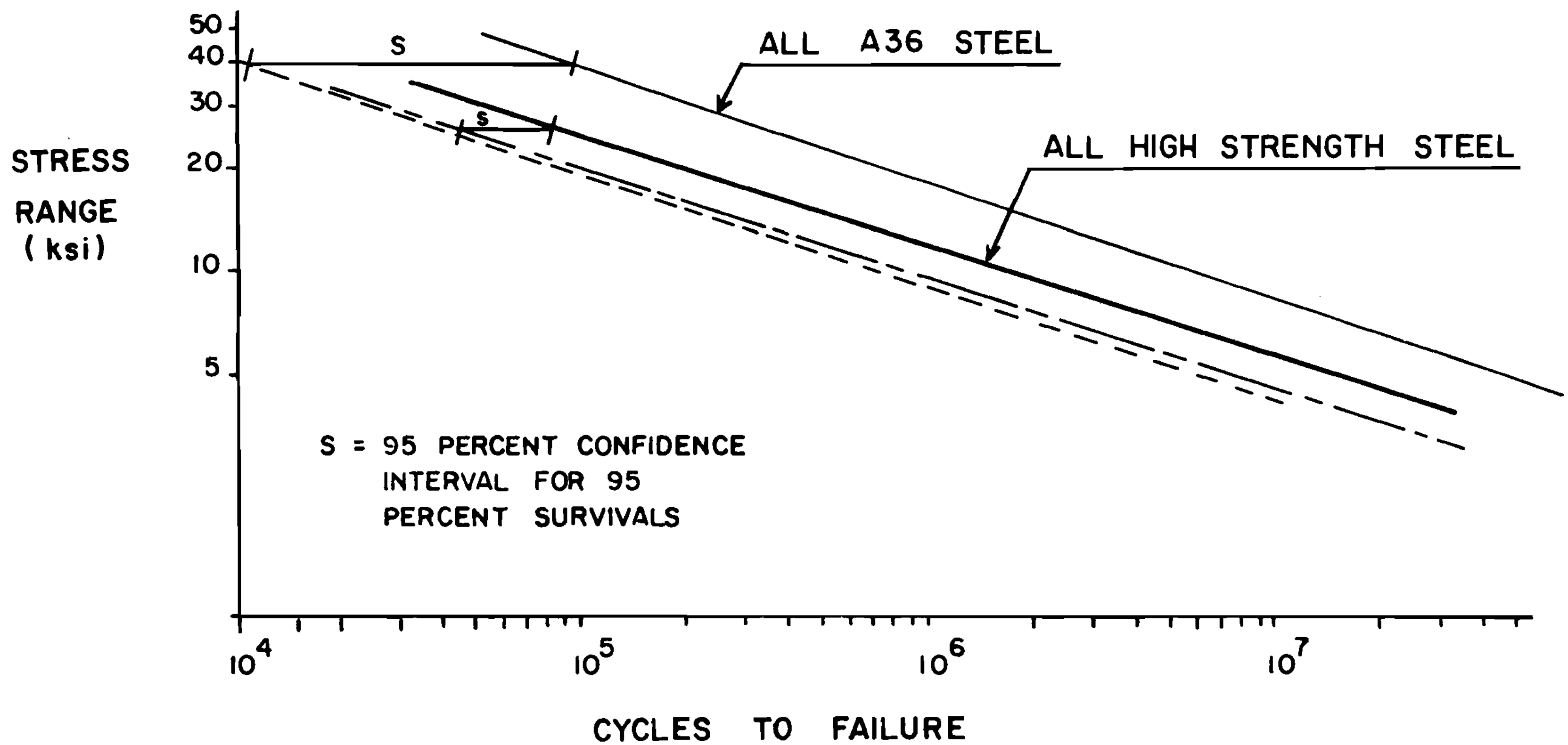

Fig. 24. Regression Lines for High and Low Strength Steels with 95 Percent Confidence Intervals.

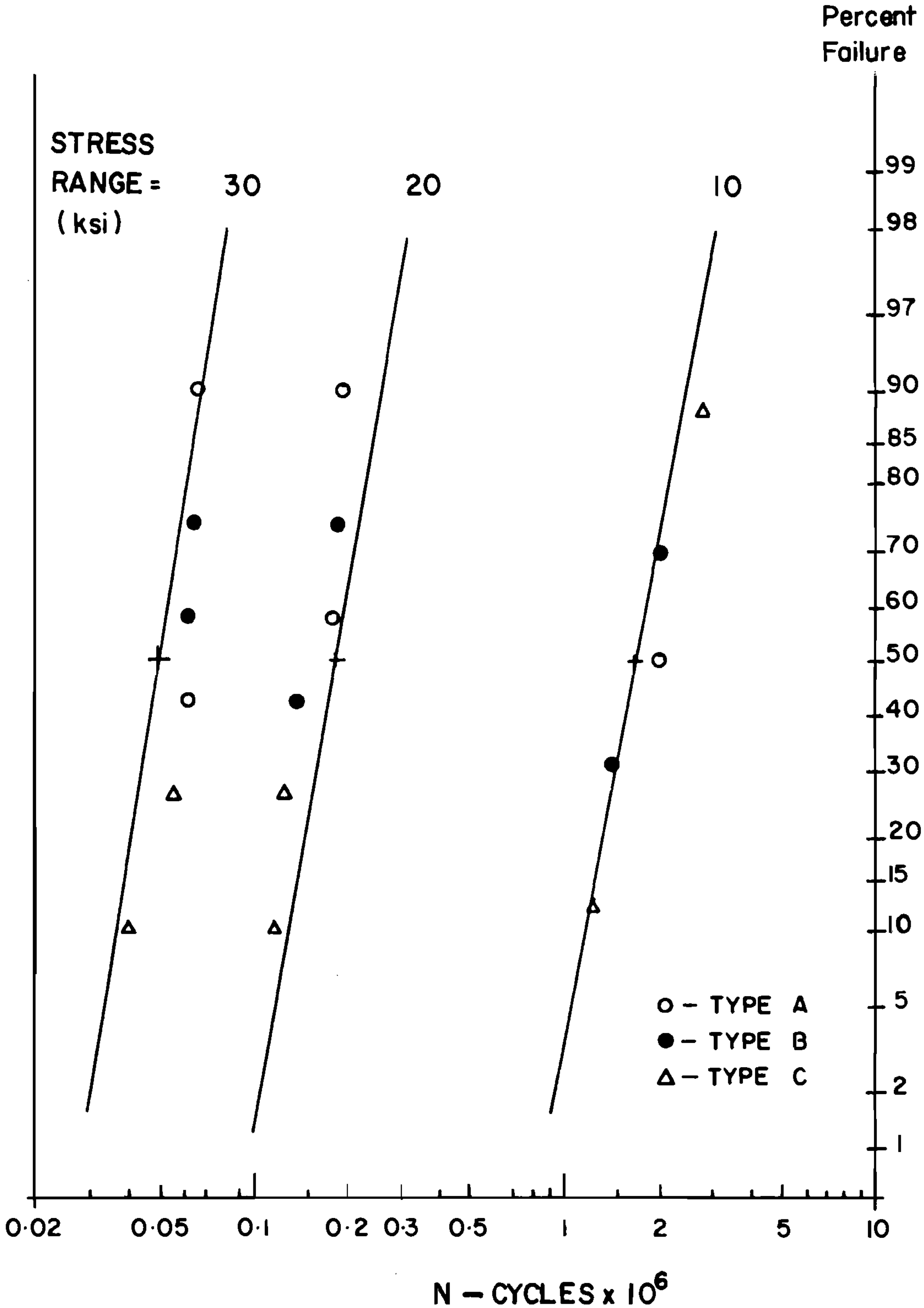

Fig. 25. Cumulative Frequency Diagram - A193 and 4340 Steels.

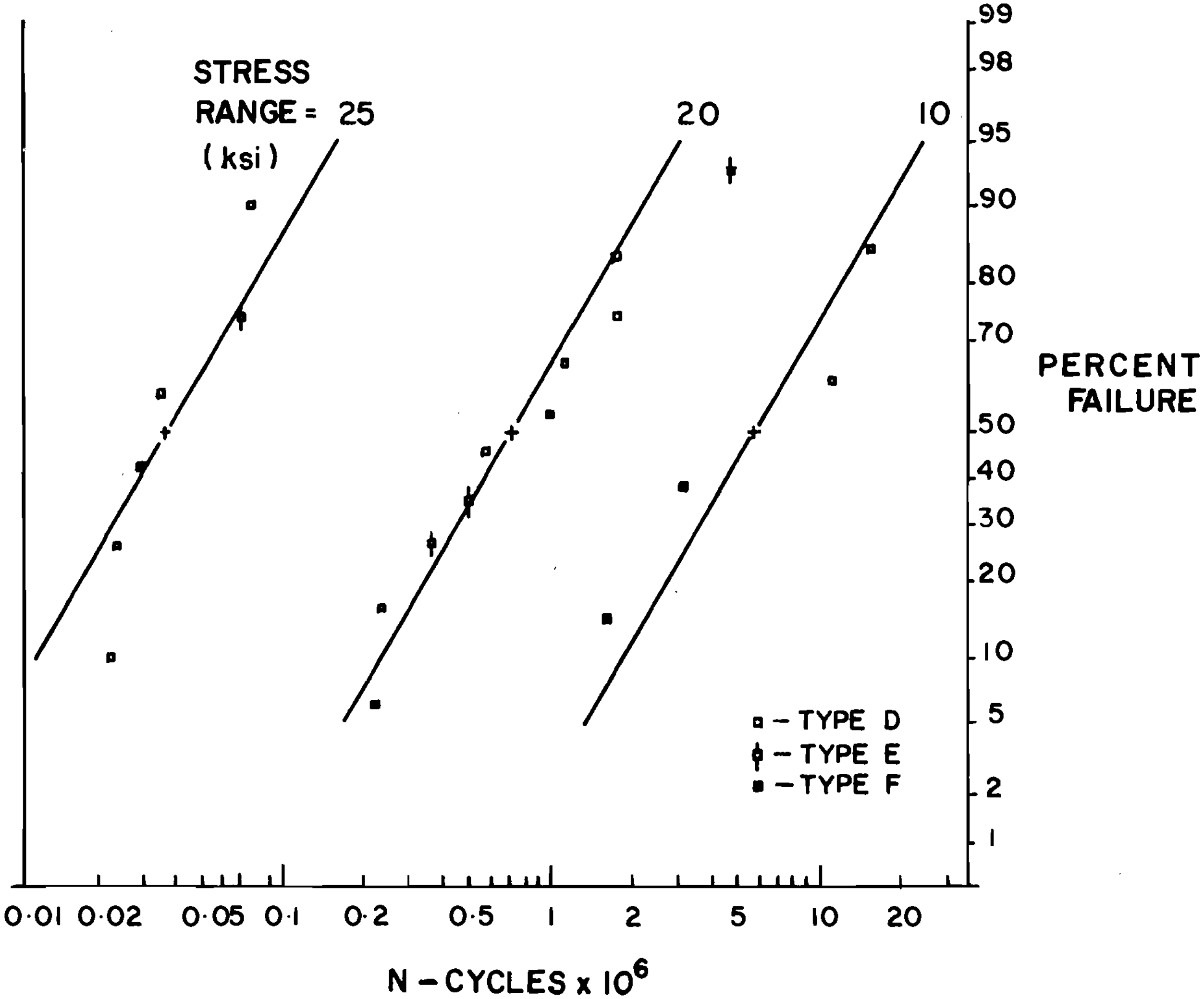

Fig. 26. Cumulative Frequency Diagram - A36 Steel.

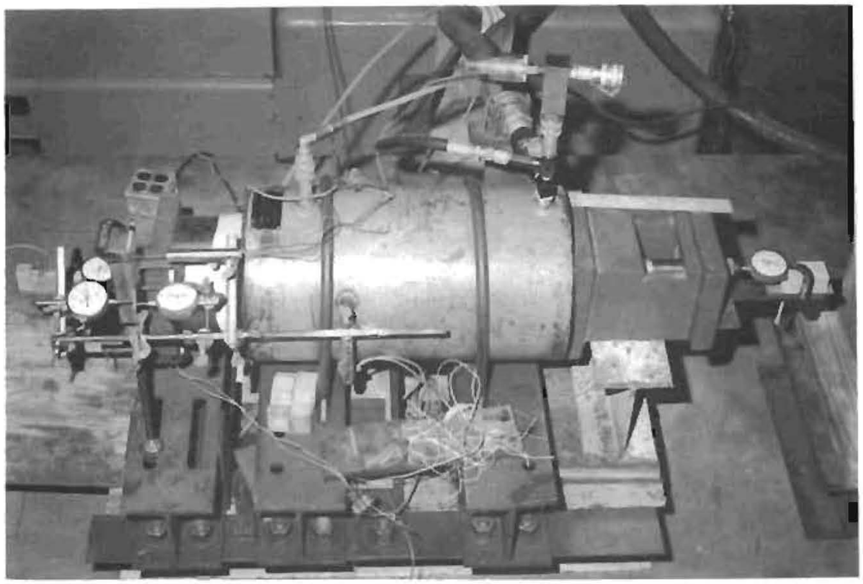

Fig. 27. Loading System for Full-sized Tension Tests.

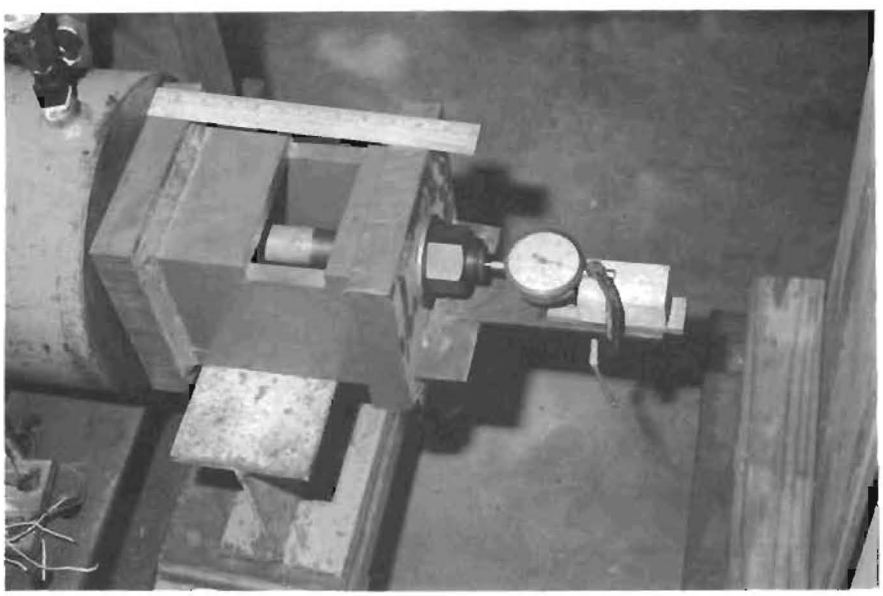

Fig. 28. Dial Gage for Nut Stiffness Measurement.

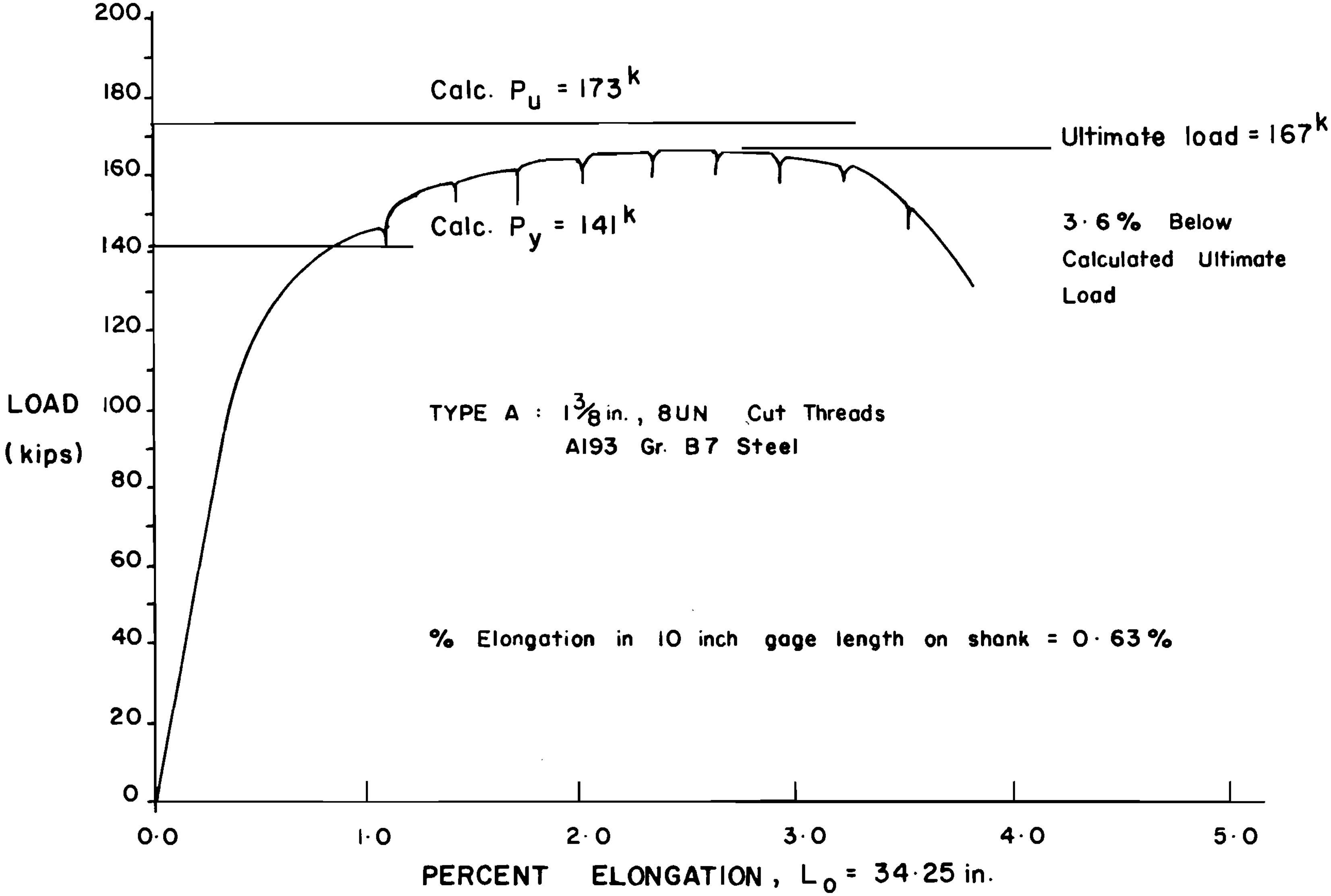

Fig. 29. Full-size Tension Test Results, Type A.

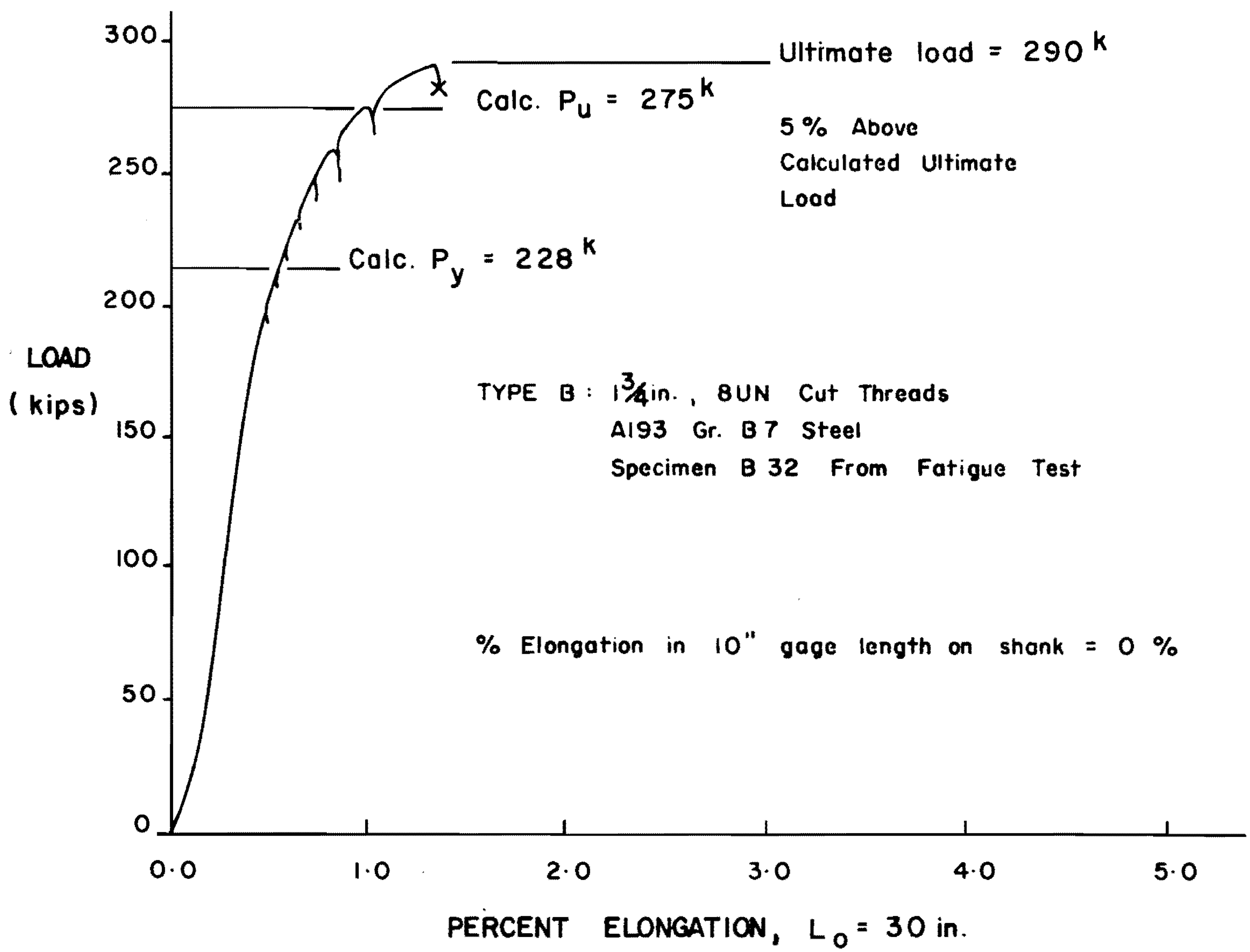

Fig. 30. Full-size Tension Test Results, Type B.

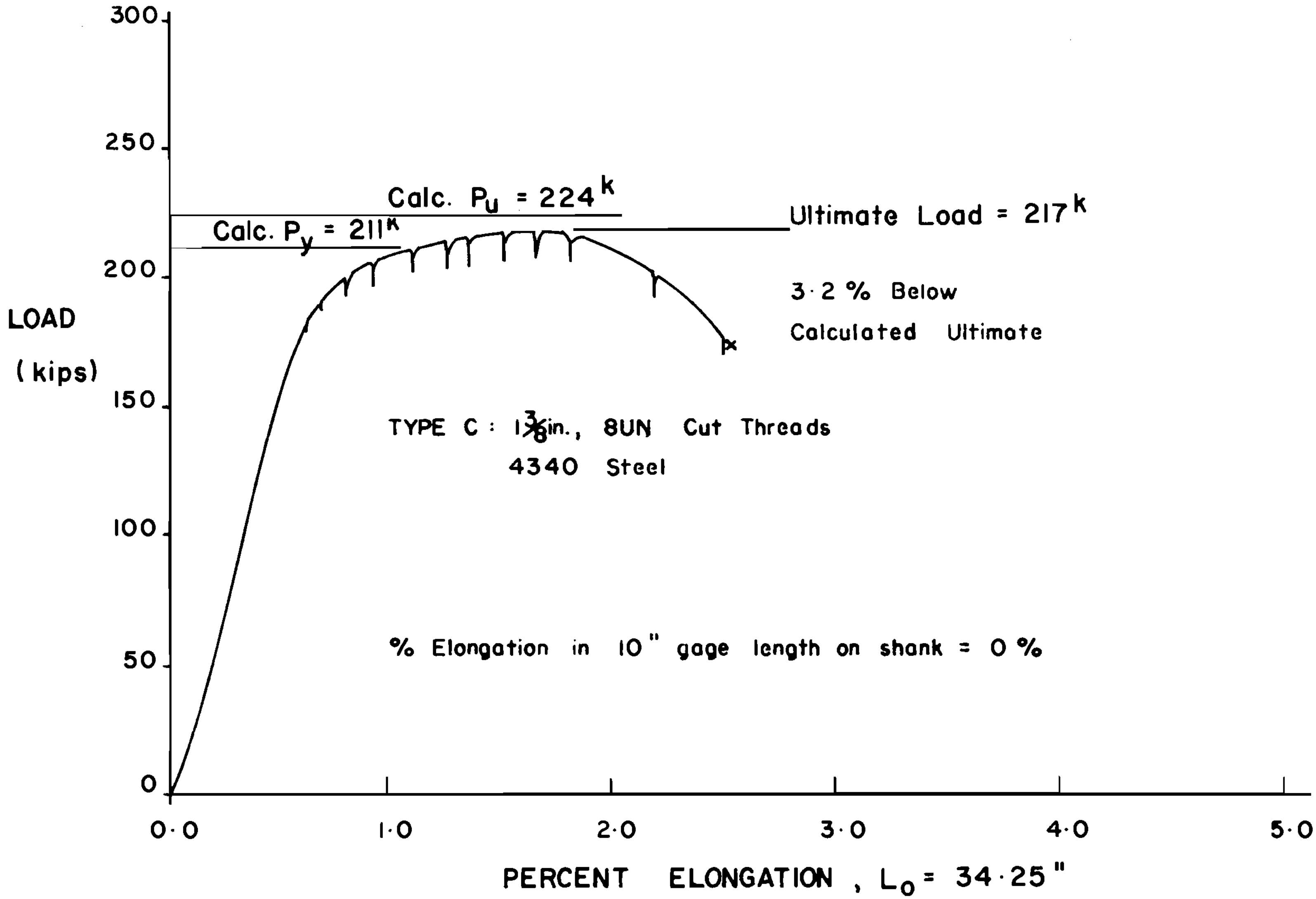

Fig. 31. Full-size Tension Test Results, Type C.

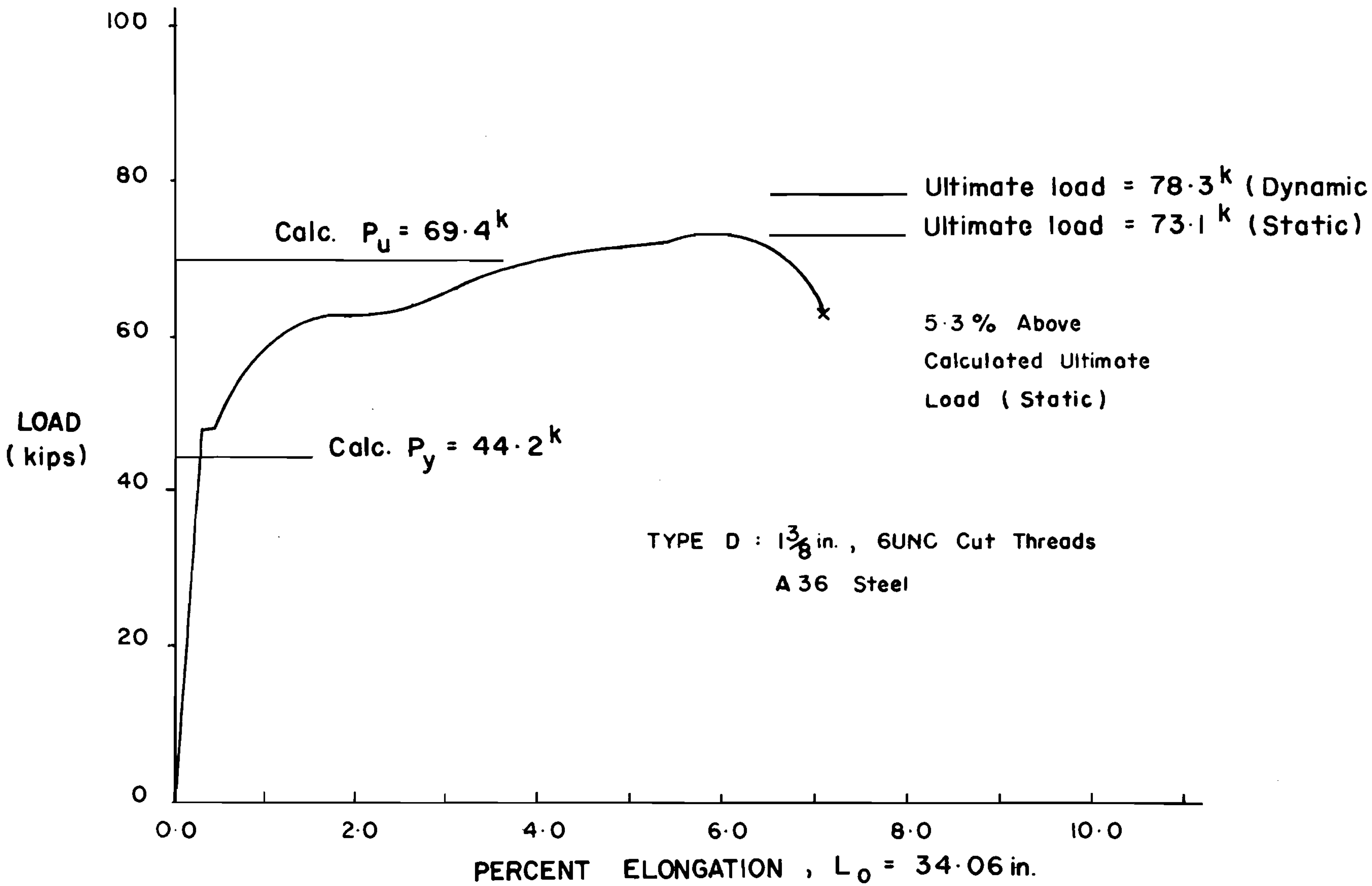

Fig. 32. Full-size Tension Test Results, Type D.

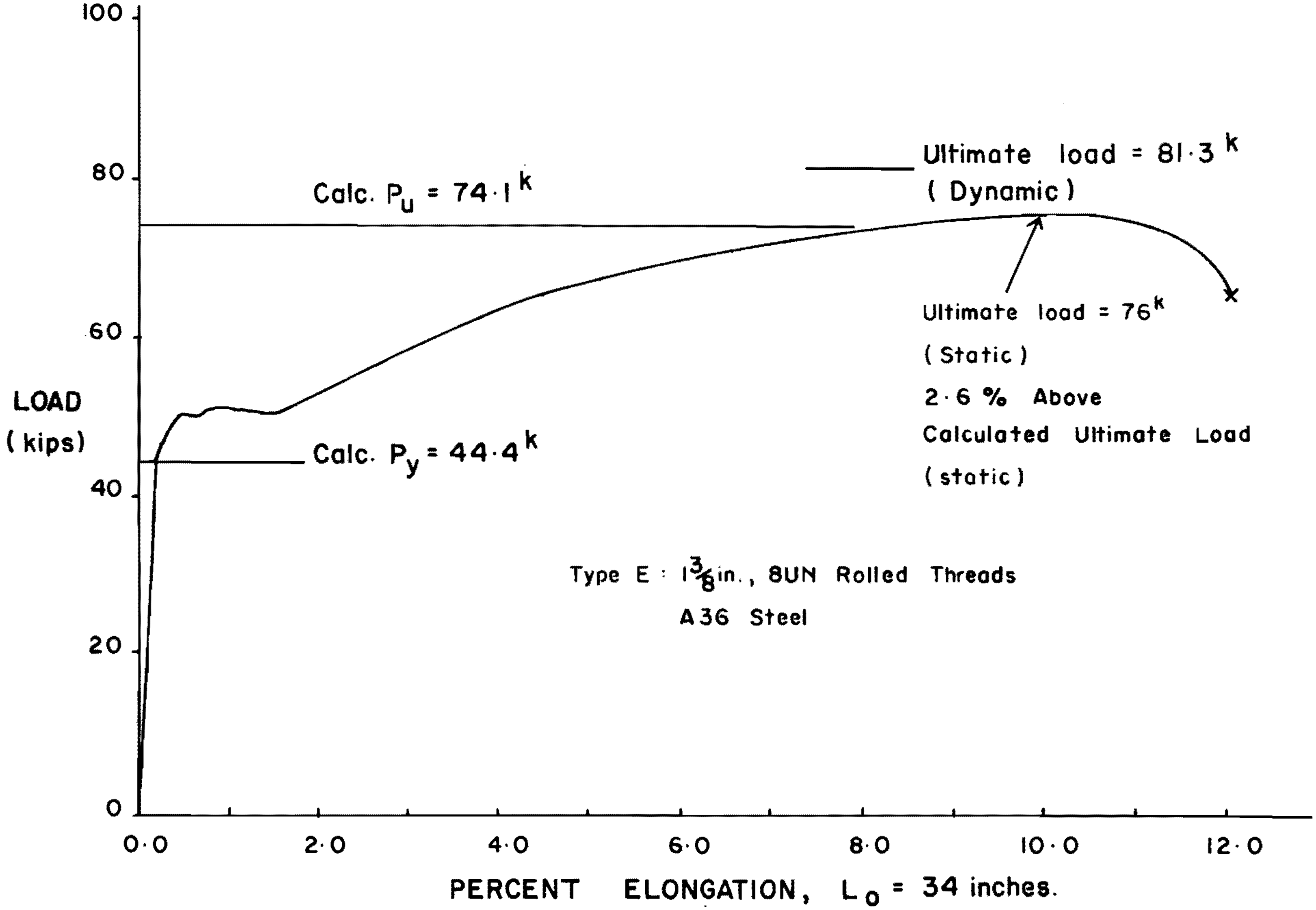

Fig. 33. Full-size Tension Test Results, Type E.

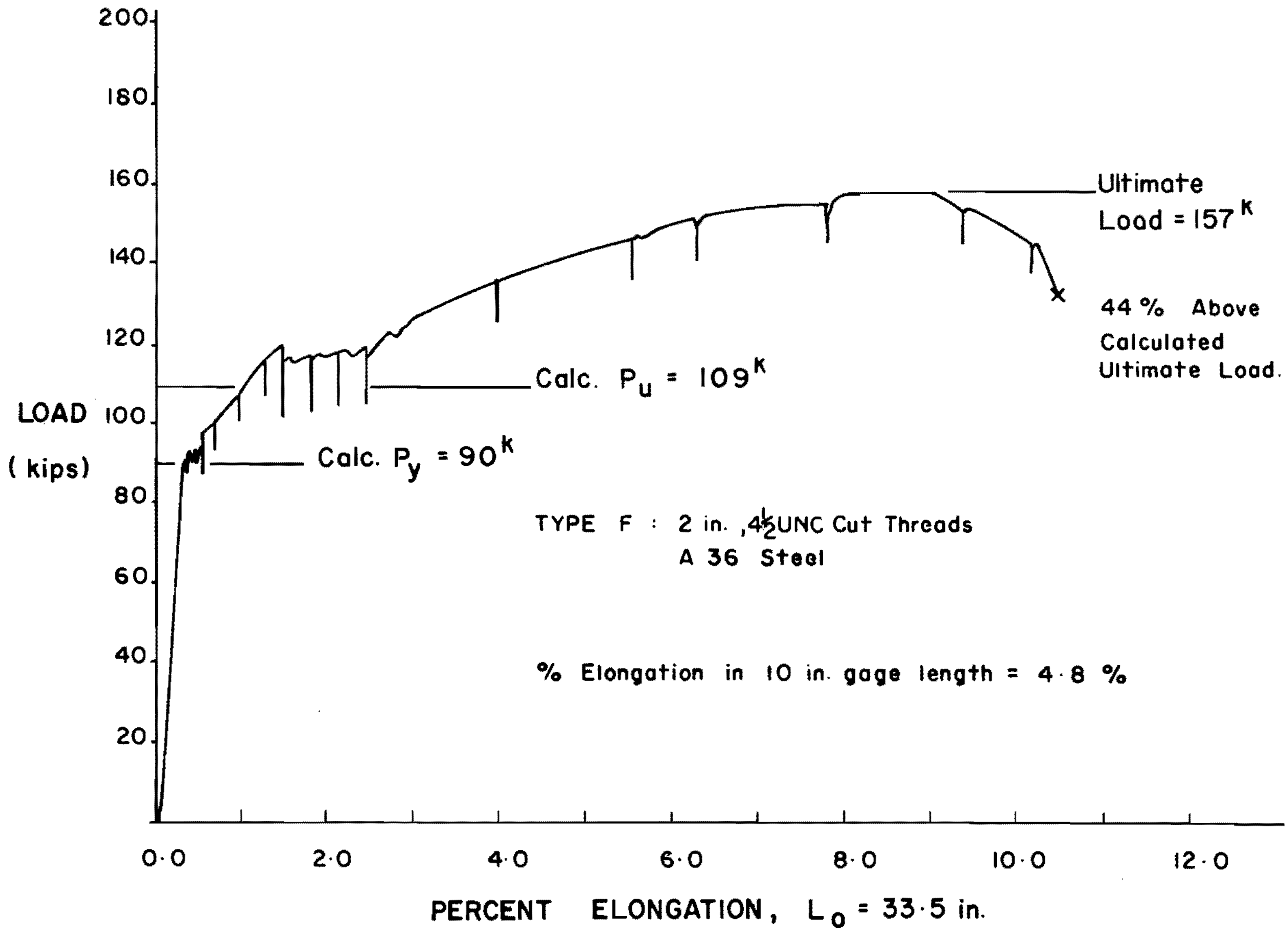

Fig. 34. Full-size Tension Test Results, Type F.

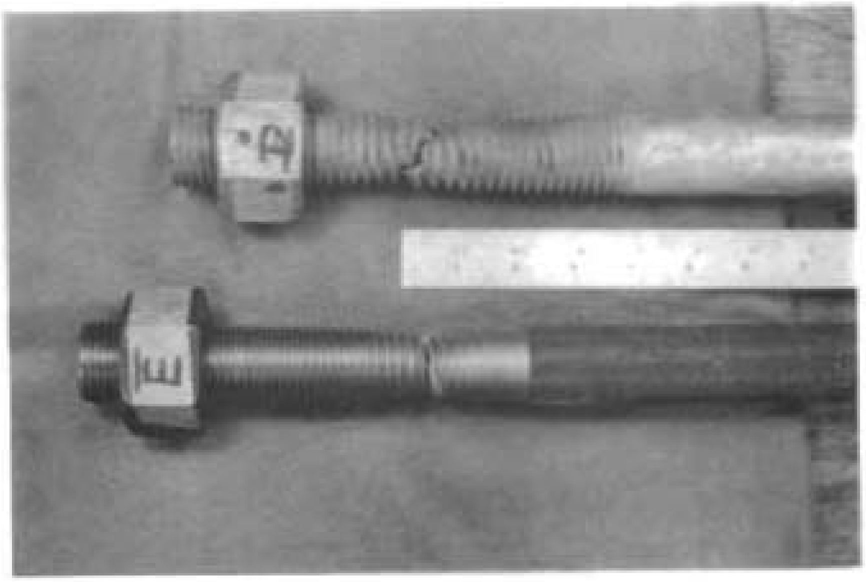

Fig. 35. Failed Full-size Tension Specimens.

Fig. 36. Charpy V-notch Low Temperature Bath Setup.

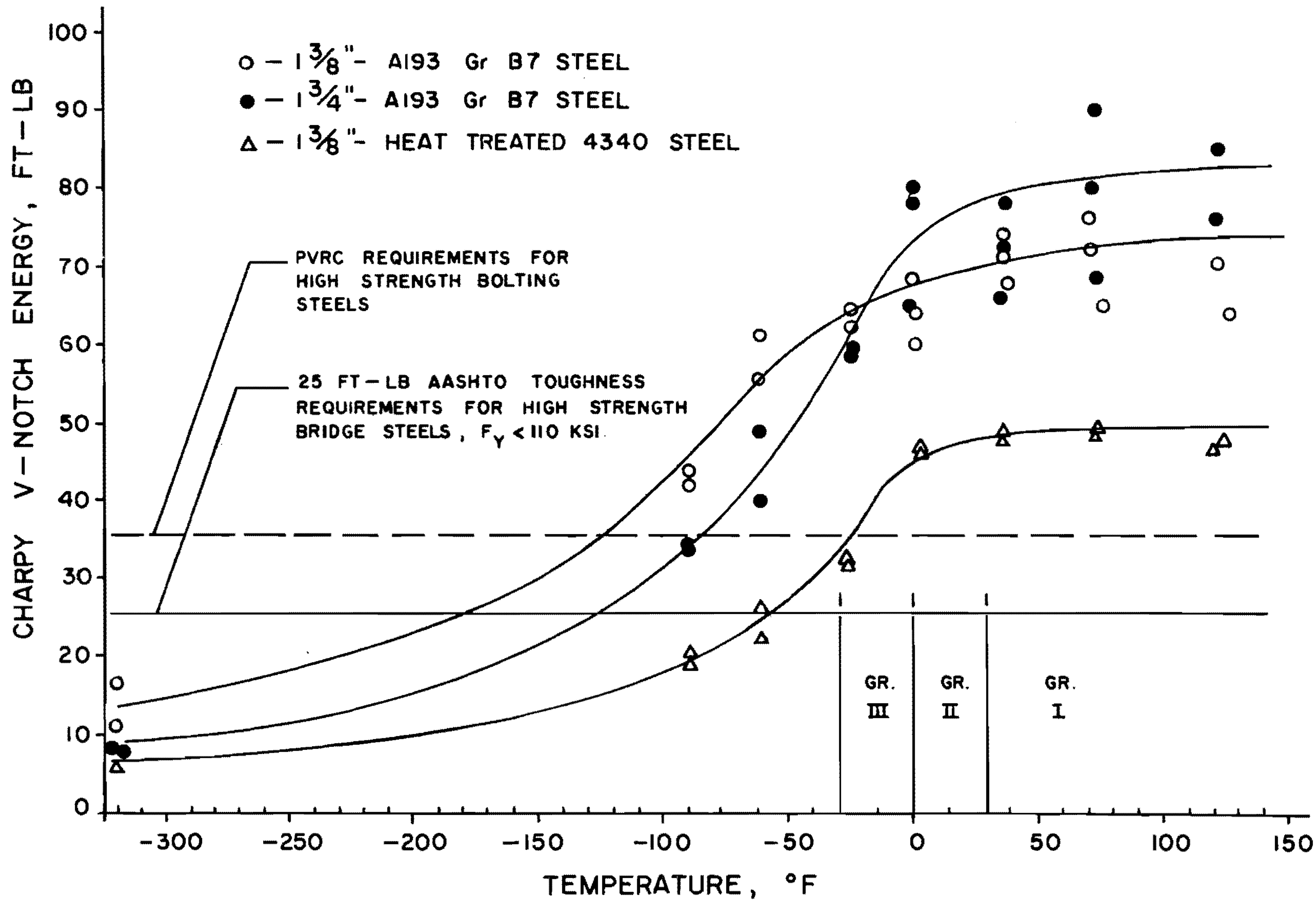

Fig. 37. Charpy V-notch Test Results for A193 Gr. B7 and Heat-treated Steel.

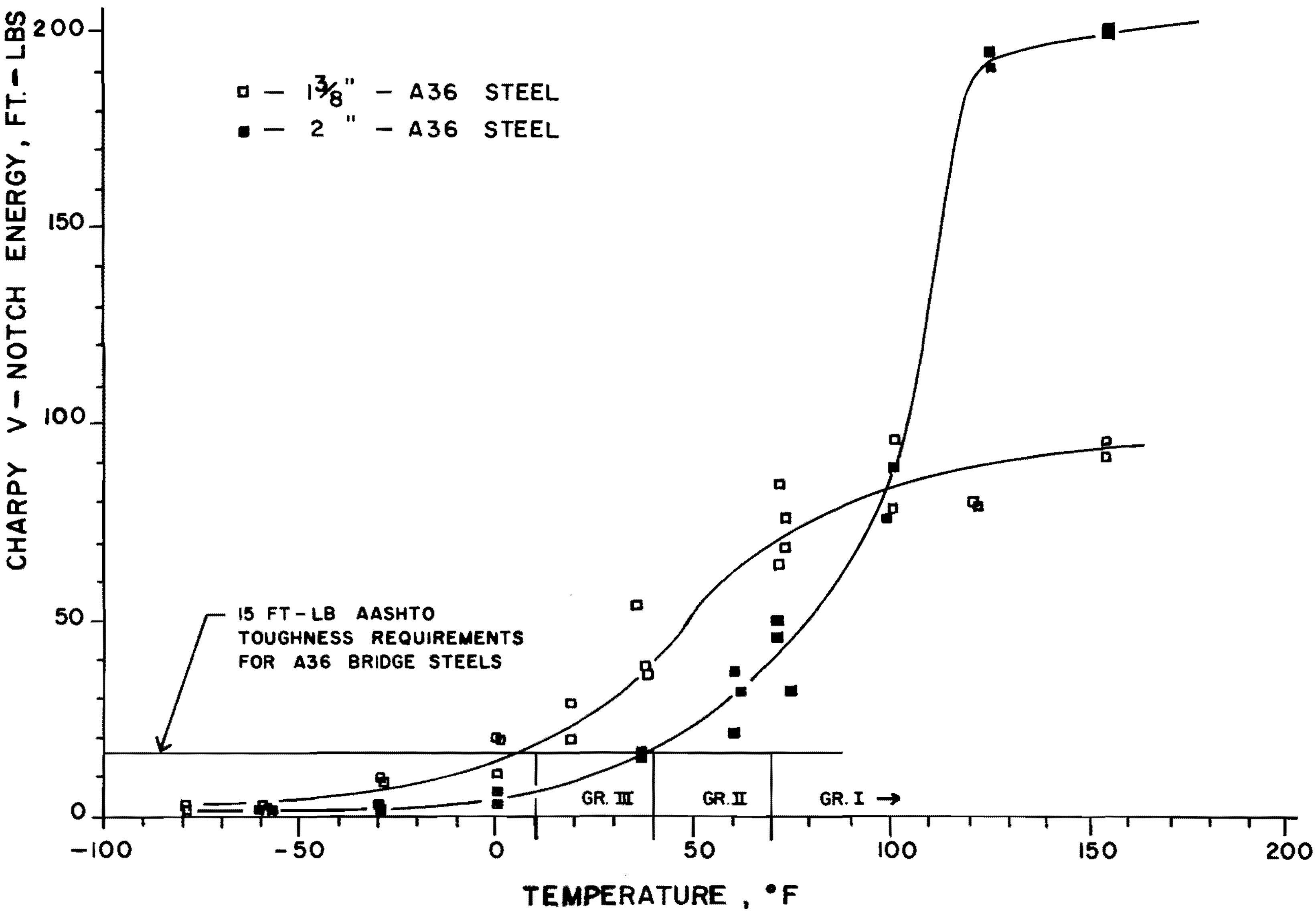

Fig. 38. Charpy V-notch Test Results for A36 Steel.

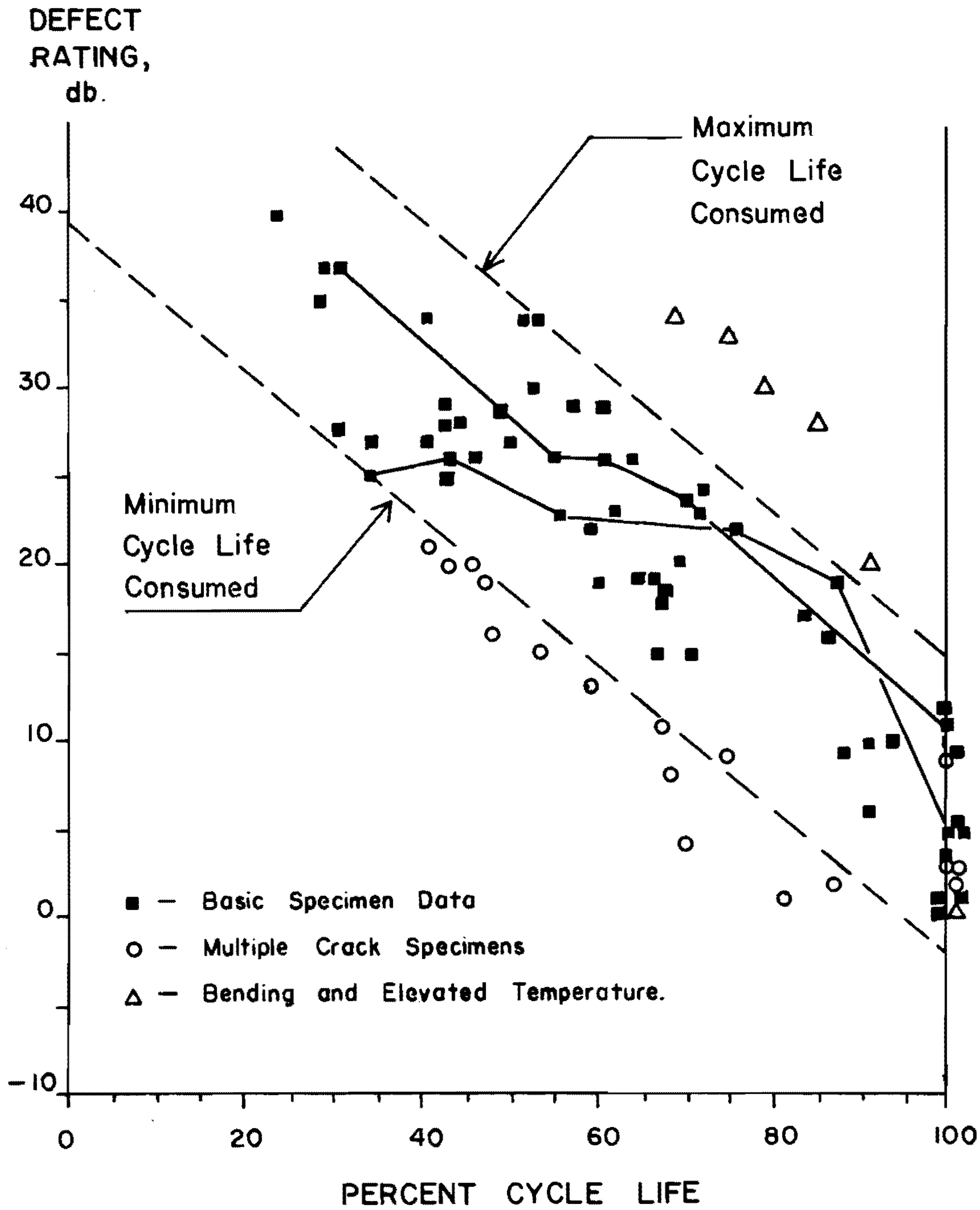

Fig. 39. Ultrasonic Inspection Results for Failed Ends.

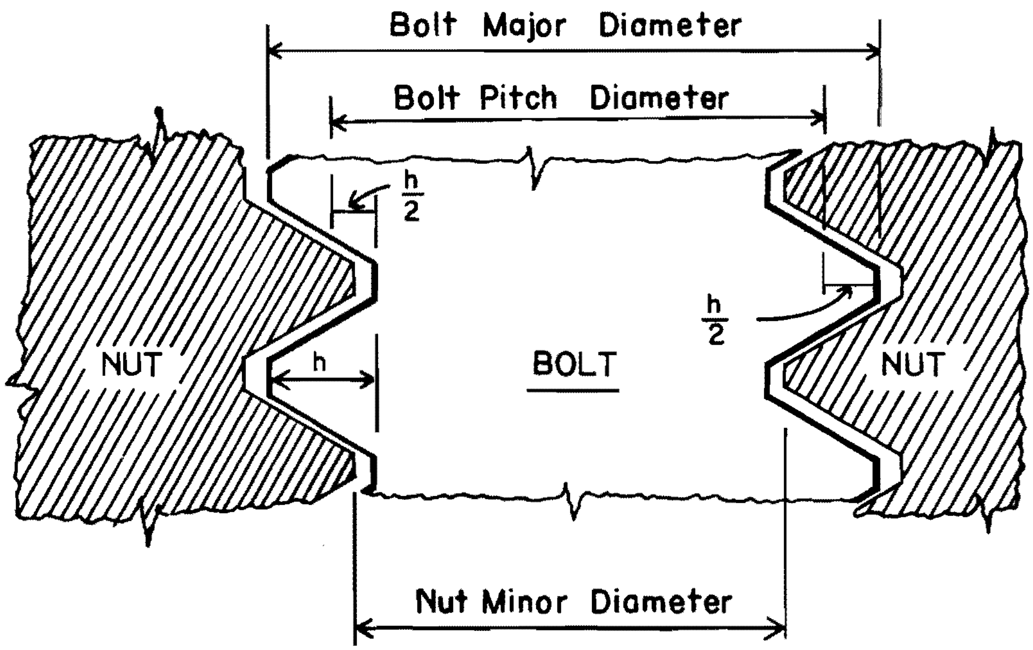

Fig. 40. Definition of Thread Diameters.

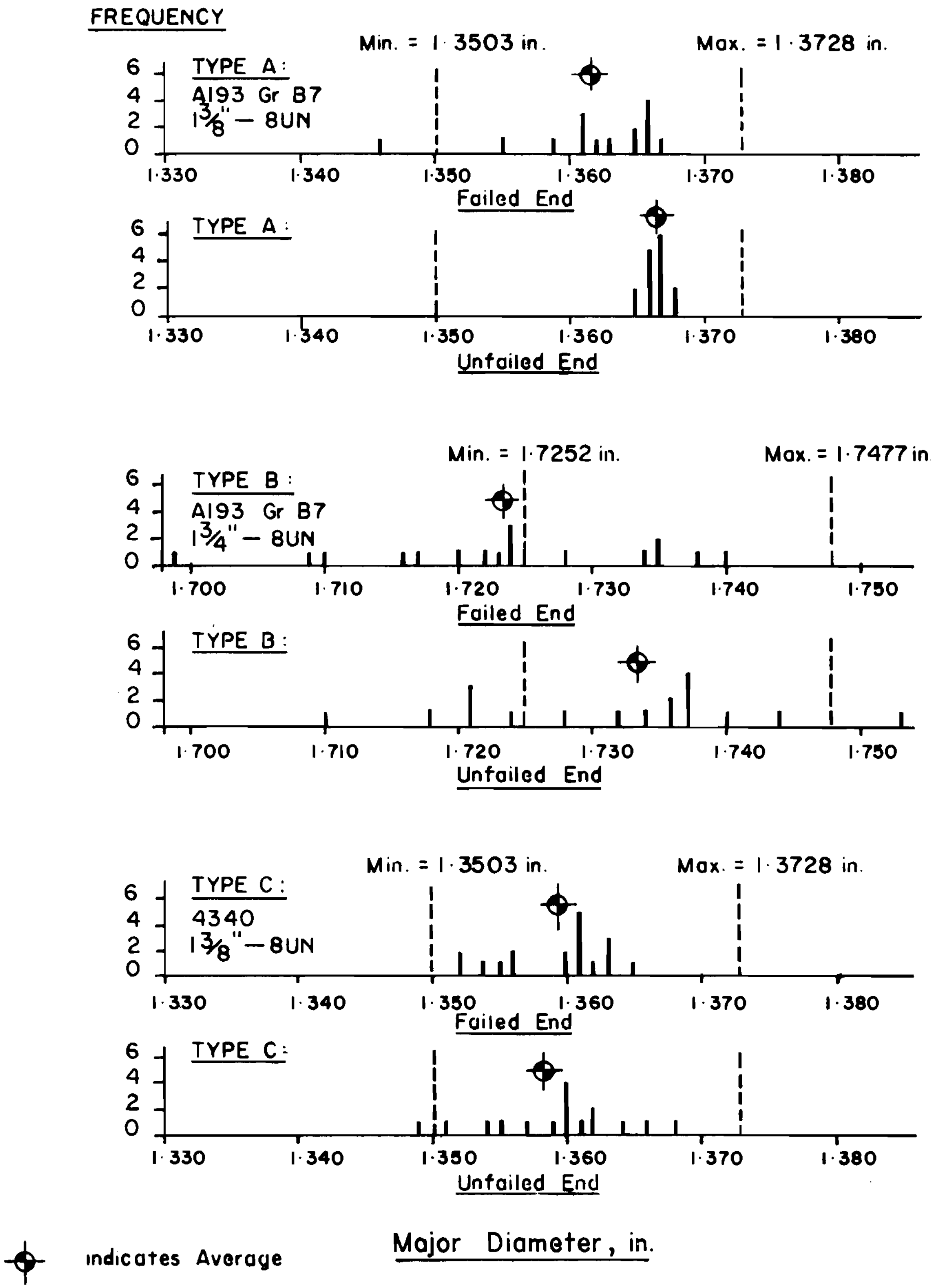

Fig. 41. Major Diameter Measurements for High Strength Steel Specimens.

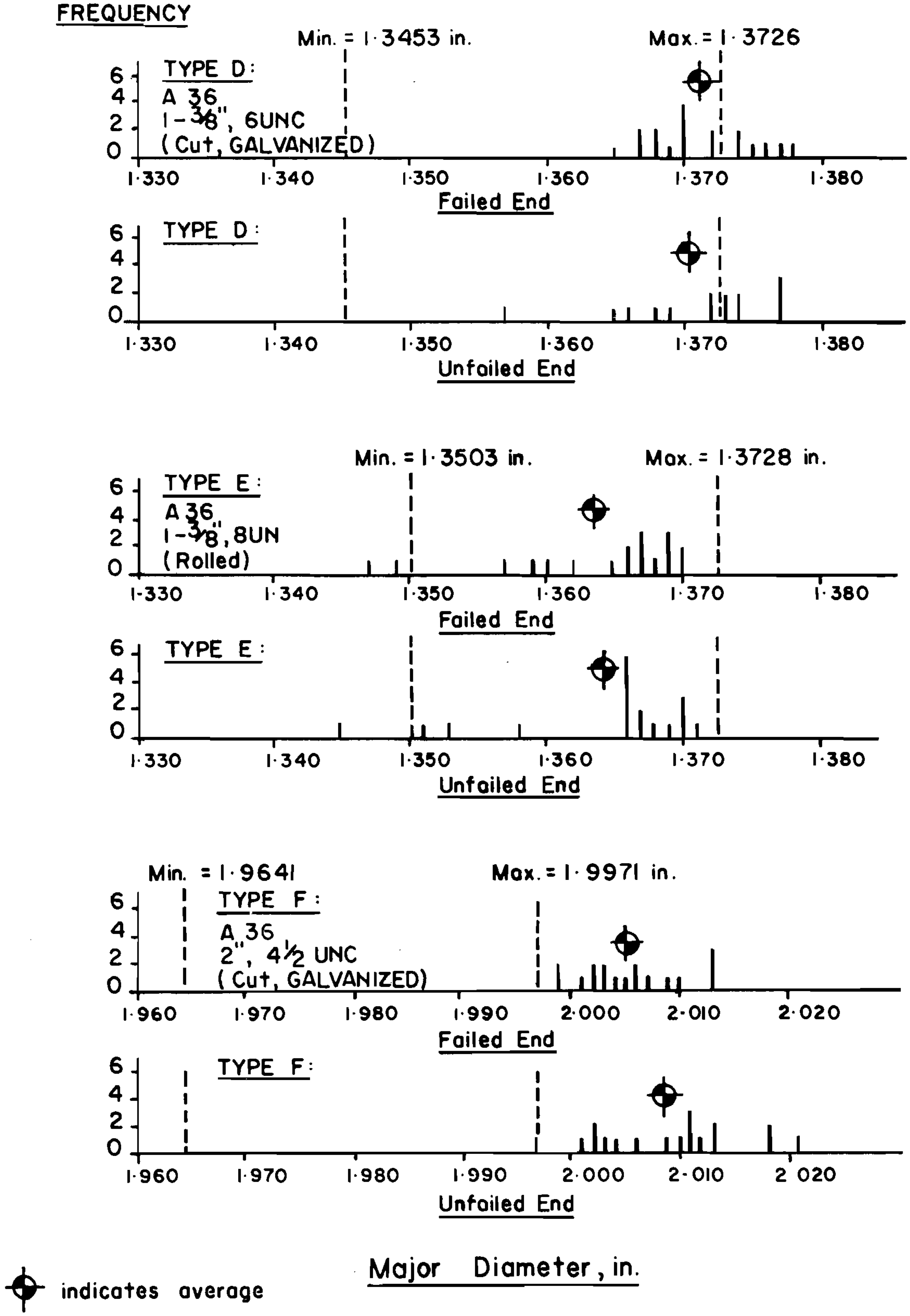

Fig. 42. Major Diameter Measurements for A36 Specimens.

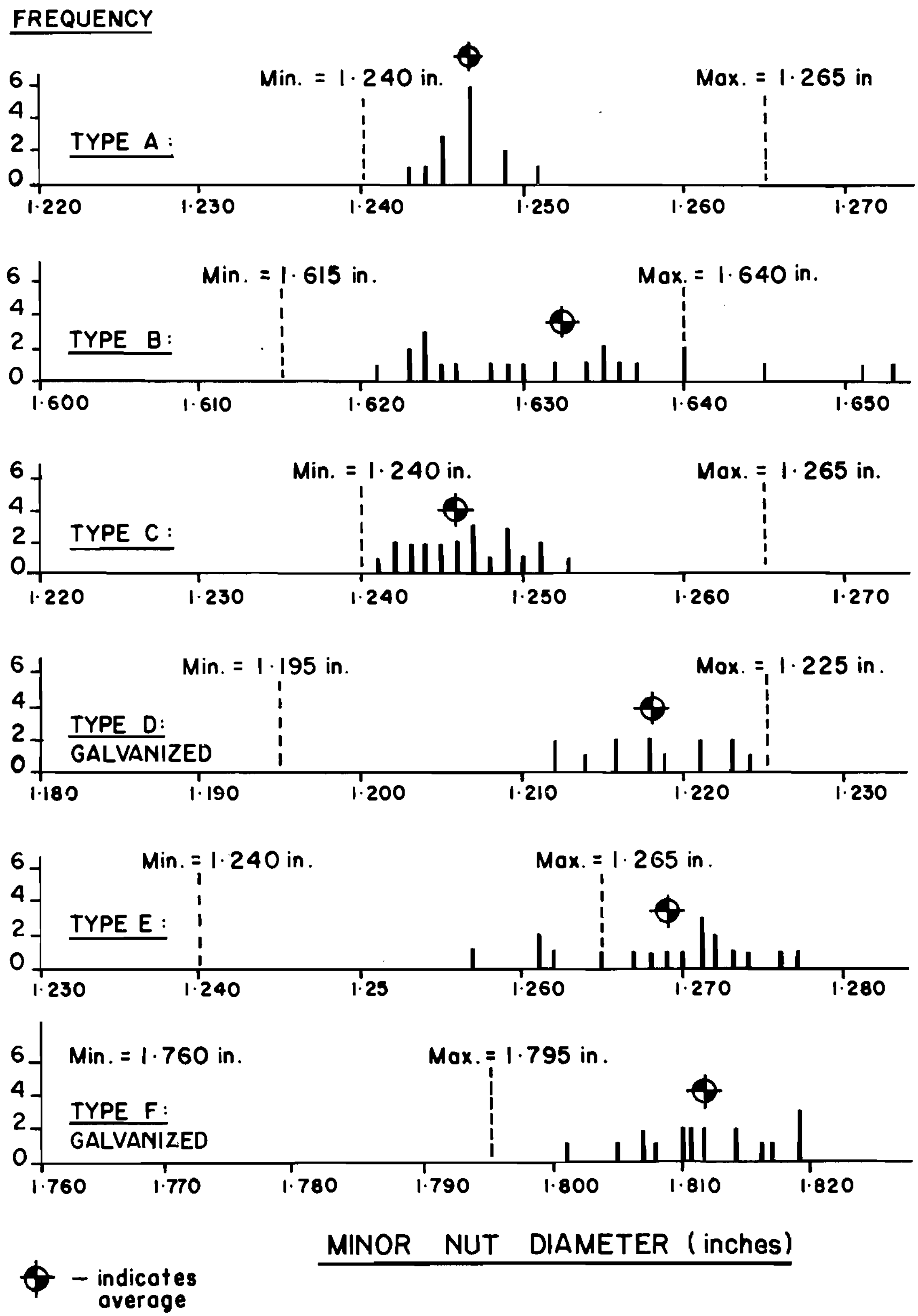

Fig. 43. Nut Minor Diameter Measurements for All Series.

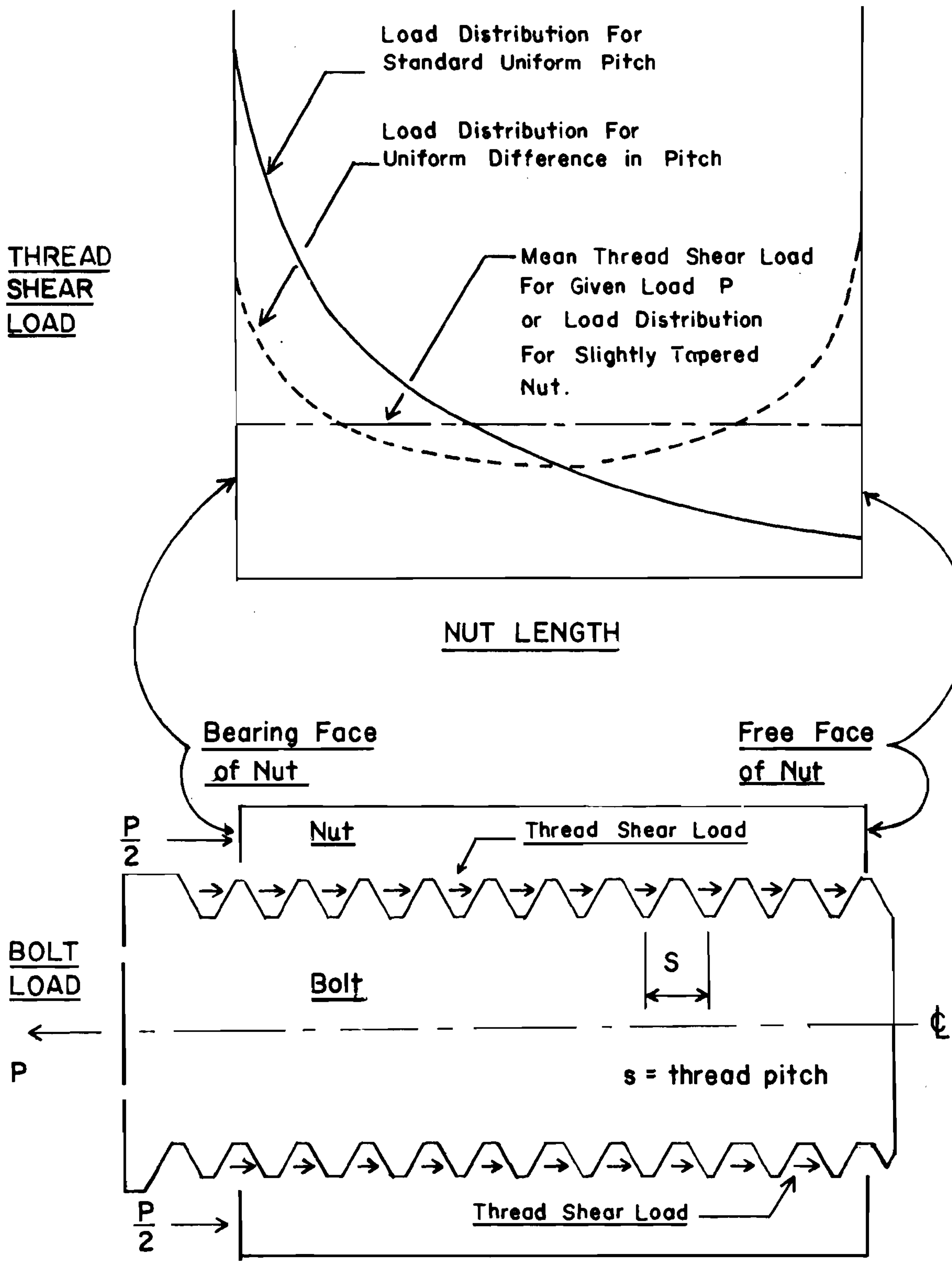

Fig. 44. Thread Shear Load Distribution and Effect of Thread Pitch.

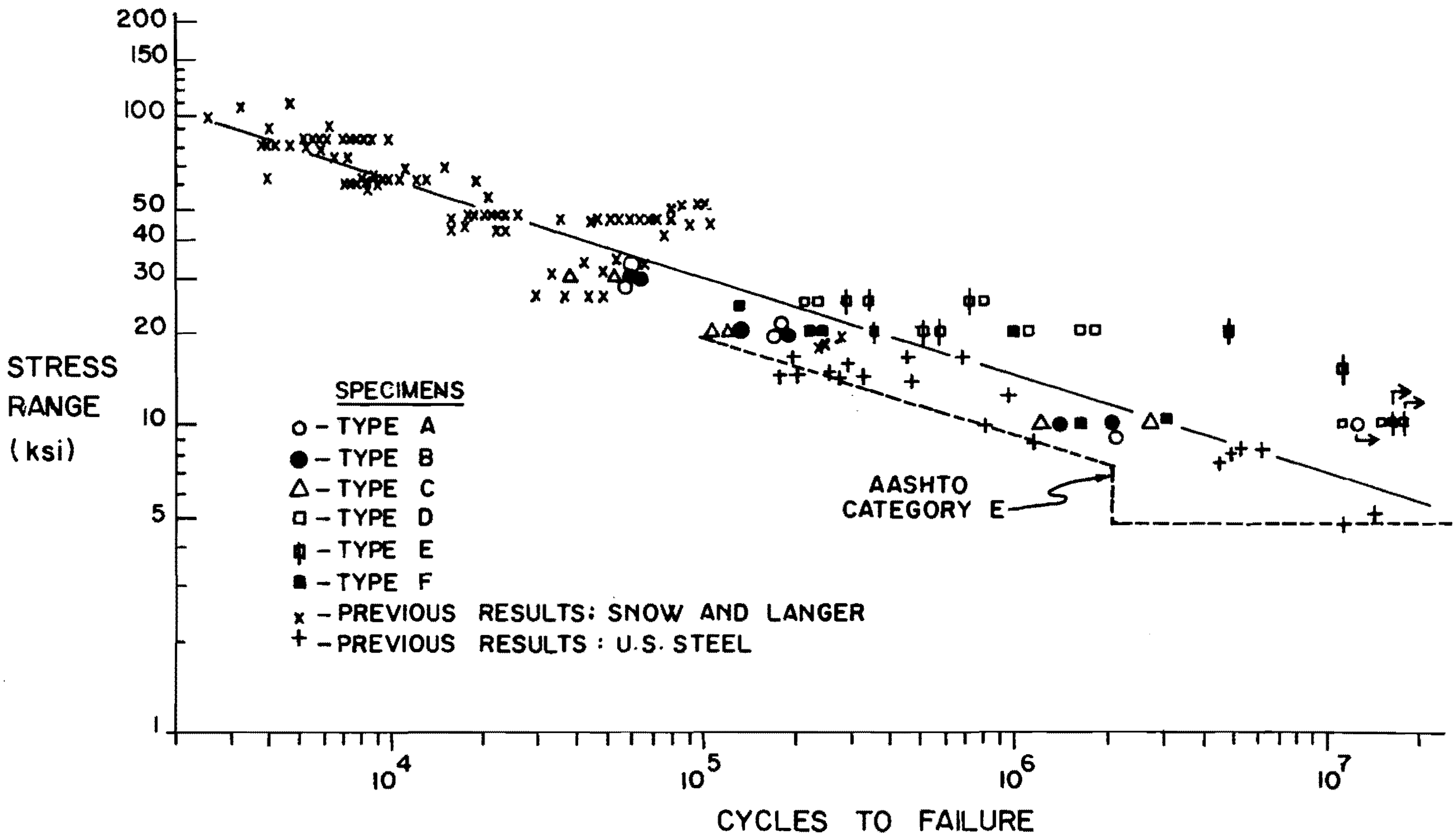

Fig. 45. Comparison of Mean Regression Line for All Test Data with Previous Test Results.

REFERENCES

1. American Association of State Highway and Transportation Officials (AASHTO) Committee on Bridges and Structures, AASHTO Material Specifications, 1973.

2. American National Standard Institute, Unified Inch Screw Threads, ANSI B1.1-1974, American Society of Mechanical Engineers, New York, 1974.

3. American Welding Society, Structural Welding Code, AWS D1.1-75, Miami, Florida, 1975.

4. Dixon, W. J., and Massey, Jr., F. J., Introduction to Statistical Analysis, McGraw-Hill, New York, 1951.

5. Handbook of Fatigue Testing, ASTM Special Tech. Pub. No. 566, S. R. Swanson, Ed., American Society for Testing and Materials, Philadelphia, Pa., 1974.

6. Heywood, R. B., "Longer Fatigue Life for Nuts and Bolts," Engineering, Vol. 189, No. 4903, April 8, 1960, pp. 494-495.

7. Iakushev, Aleksander Ivanovich, Effect of Manufacturing Technology and Basic Thread Parameters on the Strength of Threaded Connexions, Translated from Russian by S. H. Taylor, Macmillan, New York, 1964.

8. Moore, H. F., and Henwood, P. E., The Strength of Screw Threads Under Repeated Tension, University of Illinois, Engineering Experiment Station Bulletin No. 264, Urbana, Illinois, March 1934.

9. Natrella, M. G., Experimental Statistics, National Bureau of Standards Handbook 91, U. S. Printing Office, Washington, D.C. 1963.

10. "Pressure Vessel Research Committee (PVRC) Recommendations on Toughness Requirements for Fenitic Materials," Bulletin No. 175, Welding Research Council, August, 1972.

11. Reemsnyder, H. S., Estimation of Cumulative Frequency Distribution by Order Statistics for Sample Sizes 1 to 100, Files: 1414, 1712, Homer Research Laboratories, Bethlehem Steel Co.

12. Reemsnyder, H. S., "Procurement and Analysis of Structural Fatigue Data," Journal of the Structural Division, ASCE, Vol. 95, St. 7, July 1969, pp. 1533-1551.

13. Snow, A. L., and Langer, B. F., "Low Cycle Fatigue of Large-Diameter Bolts," Journal of Engineering for Industry, Trans. ASME, Vol. 89 Series B, No. 1, Feb. 1967, pp. 53-61.

14. Sophwith, D.G., "The Distribution of Load in Screw Threads," Proc. Institute of Mechanical Engineers, Vol. 159, 1948, pp. 373-383.

15. State of California Business and Transportation Agency, "Standard Specifications," Department of Transportation, January 1975, pp. 381-382.

16. United States Steel Corporation Research Laboratory, Unpublished data in private communication from J. H. Gross to K. H. Frank June 7, 1976.